

See discussions, stats, and author profiles for this publication at: <https://www.researchgate.net/publication/381813575>

Parameter Fine tuning on CRDI engine operated with blends of Grape Biodiesel and Diesel

Article *in* Case Studies in Thermal Engineering · June 2024

DOI: 10.1016/j.csite.2024.104701

CITATION

1

READS

20

12 authors, including:



[Prakash Paramasivam](#)

Vels University

11 PUBLICATIONS 27 CITATIONS

[SEE PROFILE](#)



[Hariharan Chelladurai](#)

Easwari Engineering College

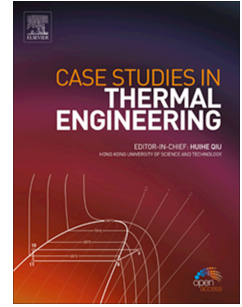
8 PUBLICATIONS 73 CITATIONS

[SEE PROFILE](#)

Journal Pre-proof

Parameter Fine tuning on CRDI engine operated with blends of Grape Biodiesel and Diesel

P. Prakash, Assistant Professor, Elumalai P.V., Research Fellow, Hariharan Chelladurai, Assistant Professor, Golden Renjith Nimal Renjith Josephine, Associate Professor, Ramesh Velumayil, Mohammad Asif, Chan Choon Kit, Balambica Venkatesan, Professor & Head, Sabarish Rajagopal, Associate Professor, Baskar Sanjeevi, Assistant Professor, M. Venkateswar Reddy, Prabhakar S



PII: S2214-157X(24)00732-9

DOI: <https://doi.org/10.1016/j.csite.2024.104701>

Reference: CSITE 104701

To appear in: *Case Studies in Thermal Engineering*

Received Date: 8 April 2024

Revised Date: 4 June 2024

Accepted Date: 13 June 2024

Please cite this article as: P. Prakash, P. Elumalai, H. Chelladurai, G.R.N.R. Josephine, R. Velumayil, M. Asif, C.C. Kit, B. Venkatesan, S. Rajagopal, B. Sanjeevi, M.V. Reddy, P. S, Parameter Fine tuning on CRDI engine operated with blends of Grape Biodiesel and Diesel, *Case Studies in Thermal Engineering*, <https://doi.org/10.1016/j.csite.2024.104701>.

This is a PDF file of an article that has undergone enhancements after acceptance, such as the addition of a cover page and metadata, and formatting for readability, but it is not yet the definitive version of record. This version will undergo additional copyediting, typesetting and review before it is published in its final form, but we are providing this version to give early visibility of the article. Please note that, during the production process, errors may be discovered which could affect the content, and all legal disclaimers that apply to the journal pertain.

© 2024 Published by Elsevier Ltd.

Parameter Fine tuning on CRDI engine operated with blends of Grape Biodiesel and Diesel

P.Prakash^{1*}, Elumalai PV^{2,3,4*}, Hariharan Chelladurai⁵, Golden Renjith Nimal Renjith Josephine⁶, Ramesh Velumayil^{7*}, Mohammad Asif⁸, Chan Choon Kit⁹, Balambica Venkatesan¹⁰, Sabarish Rajagopal¹¹, Baskar Sanjeevi¹², M. Venkateswar Reddy¹³, Prabhakar S^{14*}

^{1*}Assistant Professor, Department of Mechanical Engineering, Vels Institute of Science Technology & Advanced Studies (VISTAS), Chennai, prakash1033@gmail.com

²Department of Mechanical Engineering, Aditya University, Surampalem, India.

³Research Fellow, Faculty of Engineering. Shinawatra University, Thailand

⁴Department of Mechanical Engineering, Saveetha School of Engineering,, Saveetha Institute of Medical and Technical Sciences (SIMATS), Chennai, Tamil Nadu- 602105

⁵Assistant Professor, Department of Automobile Engineering, Easwari Engineering College, Chennai, chariharan27@gmail.com

⁶Associate Professor, Department of Mechanical Engineering, Jai Shriram Engineering College, Tirupur 638660, goldenrenjith@gmail.com

⁷Department of Mechanical Engineering, Vel Tech Rangarajan Dr. Sagunthala R&D Institute of Science and Technology, Avadi, Chennai, Tamil Nadu, India 600062.

⁸Department of Chemical Engineering, King Saud University, P.O. Box 800, Riyadh 11421, Saudi Arabia.; masif@ksu.edu.sa

⁹Faculty of Engineering and Quantity Survey INTI International University, Persiaran Perdana BBN, Putra Nilai, 71800 Nilai, Negeri Sembilan, Malaysia

¹⁰Professor & Head, Department of Mechanical Engineering, Bharath Institute of Higher Education & Research, Chennai, balambicavenkatesan.d2624@gmail.com

¹¹Associate Professor, Department of Mechanical Engineering, Bharath Institute of Higher Education & Research, Chennai, sabarish5041@gmail.com

¹²Assistant Professor, Department of Automobile Engineering, Vels Institute of Science Technology & Advanced Studies (VISTAS), Chennai, baskar133.se@velsuniv.ac.in

¹³Department of Mechanical Engineering, MLR Institute of Technology, Hyderabad, Telangana, India

¹⁴School of Mechanical Engineering, Wollo University, Ethiopia

Corresponding Email: mallevreddy@gmail.com, prabhakar@kiot.edu.et,
selvaramesh27@gmail.com, elumalaimech89@gmail.com

Journal Pre-proof

Parameter Fine tuning on CRDI engine operated with blends of Grape Biodiesel and Diesel

P.Prakash^{1*}, Elumalai PV^{4*} Hariharan Chelladurai², Golden Renjith Nimal Renjith Josephine³, Ramesh Velumayil^{12*} Mohammad Asif¹⁰, Chan Choon Kit¹¹ Balambica Venkatesan⁵, Sabarish Rajagopal⁶, Baskar Sanjeevi⁷, M. Venkateswar Reddy⁸, Prabhakar S⁹

^{1*}Assistant Professor, Department of Mechanical Engineering, Vels Institute of Science Technology & Advanced Studies (VISTAS), Chennai, prakash1033@gmail.com

²Assistant Professor, Department of Automobile Engineering, Easwari Engineering College, Chennai, chariharan27@gmail.com

³Associate Professor, Department of Mechanical Engineering, Jai Shriram Engineering College, Tirupur 638660, goldenrenjith@gmail.com

⁴Department of Mechanical Engineering, Aditya University, Surampalem, India.

⁴Research Fellow, Faculty of Engineering. Shinawatra University, Thailand

⁴Department of Mechanical Engineering, Saveetha School of Engineering,, Saveetha Institute of Medical and Technical Sciences (SIMATS), Chennai, Tamil Nadu- 602105

⁵Professor & Head, Department of Mechanical Engineering, Bharath Institute of Higher Education & Research, Chennai, balambicavenkatesan.d2624@gmail.com

⁶Associate Professor, Department of Mechanical Engineering, Bharath Institute of Higher Education & Research, Chennai, sabarish5041@gmail.com

⁷Assistant Professor, Department of Automobile Engineering, Vels Institute of Science Technology & Advanced Studies (VISTAS), Chennai, baskar133.se@velsuniv.ac.in

⁸Department of Mechanical Engineering, MLR Institute of Technology, Hyderabad, Telangana, India

⁹School of Mechanical Engineering, Wollo University, Ethiopia

¹⁰Department of Chemical Engineering, King Saud University, P.O. Box 800, Riyadh 11421, Saudi Arabia.; masif@ksu.edu.sa

¹¹Faculty of Engineering and Quantity Survey INTI International University, Persiaran Perdana BBN, Putra Nilai, 71800 Nilai, Negeri Sembilan, Malaysia

¹²Department of Mechanical Engineering, Vel Tech Rangarajan Dr. Sagunthala R&D Institute of Science and Technology, Avadi, Chennai, Tamil Nadu, India 600062.

Email: mallevreddy@gmail.com, prabhakar@kiot.edu.et, selvaramesh27@gmail.com, elumalaimech89@gmail.com

Abstract

This study investigates the feasibility of using grape biodiesel from the wine industry as a sustainable and cost-effective alternative to traditional fuels. The research focuses on optimising key parameters like blend ratio, injection timing, injection pressure, engine load, and exhaust gas recirculation in a Common Rail Direct Injection engine to achieve low emissions without compromising performance. Due to grape biodiesel's higher viscosity, different energy content, and varying ignition delays compared to diesel, precise adjustments are essential for complete combustion and reduced emissions. This study uses response surface methodology and a Central Composite Design matrix to find the best values for a number of parameters in modern CRDI engines that use advanced electronic control units. Through fifty input combinations, the study aims to minimise specific fuel consumption, hydrocarbons, nitrogen oxides, and carbon monoxide while maximising brake thermal efficiency, brake mean effective pressure, and mechanical efficiency. The optimal configuration includes a fuel injection timing of 6° bTDC, an engine load of 82%, 6.7% EGR, 1000 bar injection pressure, and a 33% grape biodiesel blend. These optimum input conditions yielded outputs of 3.55 bar BMEP, 31.85% BTE, 64% mechanical efficiency, 0.278 kg/kWh SFC, 0.127% CO, 357 ppm NO_x, and 8 ppm of HC. These adjustments ensure low emissions and efficient engine operation, highlighting grape biodiesel's potential as a viable alternative fuel.

Keywords: optimization; CRDI engine; Biodiesel; Performance and emission characteristics; ANN; RSM, Pollution

Nomenclature

CRDI -Common rail direct injection

ECUs -Electronic control units

CCD - Central composite design

RSM - Response surface methodology

BTHE, BTE - Brake thermal efficiency

BMEP - Brake mean effective pressure

SFC - Specific fuel consumption

HC - Hydro carbon

CO - Carbon monoxide

NO_x, NO - Nitrogen oxides

ANN - Artificial neural network

IC - Internal combustion

CCRD - Central composite rotatable design

DOE - Design of experiment

B25 - Biodiesel 25% + diesel 75%

B50 - Biodiesel 50% + diesel 50%

B70 - Biodiesel 70% + diesel 25%

FB - Fuel blend

FIT - Fuel Injection timing

FIP - Fuel Injection pressure

bTDC - Before top dead center

CR - Compression ratio

EL - Engine load

BP - Brake power

BMEP - Brake mean effective pressure

EGR - Exhaust gas recirculation

GSB - Grape seed biodiesel

ppm – parts per million

exp - Experiment

Introduction

To protect human beings, animals, and all living organisms, forest areas of the plantation should be maintained or switched over to the use of low polluting substances as utmost priority for maintaining environment pollutions within limits or at least in human circumstances. Global warming and ozone layer depletion are mainly due to the emission of stringent pollutants into the atmosphere caused by transportation vehicles and industry outlets. To avoid rapid global warming and ozone layer depletion, it is an urge to use biodegradable biofuel as compression ignition engine instead of the majority of crude oil-derived diesel fuels in the way to reduce dependency on other countries for crude oil fuel, increase economic growth in the competitive environment, supply biofuel at a nominal rate than diesel, increase employability level and an income of the farmers.

Generally, IC engines are mainly used in agriculture, heavy transportation, power production, and some household applications. Also, due to the increase in population, the necessary activity of internal combustion engine application increases, causing demand for internal combustion engine fuels. Hence before exhausting the crude oil-based fuel, there is an urge to find an alternative. It is

more beneficial to find out alternative energy in a blended form with crude oil derived or in neat biodiesel by considering the engines' operating constraints.

Almost recently, researchers tried to utilize all plant sources or animal fat-derived fuels and concluded their result, such as biofuel output responses mainly depends on the nature of the biofuel source, the composition of fuel properties like kinematic viscosity, density, calorific value, cetane number, iodine value, pour point, saponification value. The fatty acid value is mainly influenced by fuel fatty acid components such as saturated, unsaturated, monounsaturated, and polyunsaturated. so based on fatty acid profile composition, it easily predict the fuel properties and is also used to choose the optimum catalyst concentration, the molar ratio of alcohol and raw oil, operating temperature, stirring speed and time for the transesterification process. To avoid clogging, degumming, and sedimentation caused during long time storage and winter climatic conditions and to improve biodiesel quality, the transesterification process is usually followed due to its advantageous nature over other techniques like thermal cracking, etc. Based on the report of a biofuel researcher, saturated dominant biodiesel fuel has a poor cloud point than unsaturated fuel. Generally, unsaturated fatty acid dominant fuel has better cloud point but both cloud and pour point of used fuel is one of the criteria to decide. So equal saturated and unsaturated fatty acid content fuels are advised to use in diesel engines to avoid climatic-based engine problems.

Biodiesel yield is mainly influenced by the type of catalyst and their proportion, time of operation, and alcohol concentration. Many researchers from chemical engineering backgrounds concentrated on these parameters and found the optimum variable combination for different biodiesel by following the design of the experiment. Recently statistical analysis-based parameter optimization is followed in preparing biodiesel from different sources and engine-influencing parameters.

The grape seed contained 15.8% of oil content and used CCRD-based DOE. Then due to the low free fatty acid nature of *Vitis vinifera* oil, following single step transesterification process revealed the optimum input combination for yielding 97.7% of biodiesel as 1.045 g of sodium hydroxide, the molar ratio of 0.2758 volume basis, 66.6 minute of reaction duration with a constant speed of 450 rpm and the temperature of 60°C (Venkatesan, A, and Sivamani 2022). Optimised the input parameters of chemical reactions used the ANN, RSM, and ANFYS to predict the output response of biodiesel yield and revealed that in the aspect of prediction ANN, ANFIS is better than RSM

(Hariram, Bose, and Seralathan 2019). By following the catalytic cracking process, evaluated the white grape seed biodiesel and the direct injection diesel engine performance was evaluated at 17.5:1 compression ratio, 1500 rpm, 215.7 bar injection pressure, 23°bTDC, and concluded that B25 Grape seed biodiesel blend BTE is similar to diesel fuel, SFC at full load for B25, B50 identical to diesel fuel and the remaining outcome of CO, HC & smoke increases except for NOx when the blending increases (Sreedhar and Durga Prasad 2015). An effective way to reduce dependency and energy demand is the production of biodiesel from vegetable oil. The feasibility of grape seed, Philipping tung, and Kesambi biodiesel by comparing these properties with palm biodiesel revealed that GSB possesses the highest oxidation stability of 4.62 hours than philipping, kesambi biodiesel. Oxidation stability further improved to 6.24 hours by adding 0.2 wt % of pyrogallol antioxidant, but for the remaining fuel, a higher wt % of antioxidant required to improve the stability. GSB contain primarily unsaturated fatty acid, and GSB, Philippi blend met the ASTM standard until 50% blend (Ong et al. 2020). B25 of GSB blend in a deep bowl combustion chamber is a better option than a standard piston combustion chamber and toroidal combustion chamber in terms of better combustion performance and emissions; however, changing other engine parameters may be experimented with for better use of GSB (Sankar Ganesh, Ganesh Babu, and Karu 2019). In 4 cylinder 4-stroke diesel engine, B70 GSB, given better performance in terms of maximum power and minimum emissions and fuel consumptions, also used a novel ANN to predict optimum blend ratio. It is a reliable alternative source to produce quality biodiesel (Fadairo and Ip 2021). GSB5, 10% and waste cooking biodiesel 5%, 10% were investigated in 4-cylinder engines and reported that due to less ignition delay, GSB5% is better in terms of performance and combustion (Azad and Rasul 2019). IT and IP play the main role in engine performance and emissions. Investigated by varying IP 275-1000bar, IT 6°bTDC to 5.5°ATDC. Early injection leads to high NOx, and also at high IP, delay time decreased, and maximum energy was released (Raeie, Emami, and Karimi Sadaghiyani 2014). DOE-based RSM techniques help reduce the number of experiments required. For a single cylinder direct injection diesel engine using B20 neem biodiesel as fuel, the optimum input combination was 225bar IP, 23°bTDC, 18.5CR (Sathiyamoorthi et al. 2019). Heterogeneous catalysts are used for the production of biodiesel from Jatropha and the input parameter considered is FIP, CR, and EL for getting maximum BP, BTE and minimum NOx, HC. Finally, the optimum factor is 18 CR, 180bar FIP and 8.11kg EL (A. Singh, Sinha, and Choudhary 2021). Simulation analysis was done by varying CR (12-16.5), FIP (500-1400bar), IT (0-

30°bTDC) and EGR (0-25%) based on DOE. Increasing CR, FIP and advancing IT turns into NO_x, and peak pressure increases except for soot. The optimum combination for favorable peak pressure, NO_x, and soot were CR14.25, FIP 1153.15bar, IT 13.69°bTDC, and EGR 16.91% (Ganji et al. 2017). All the blends of B10, B15 and B20 GSB compared with diesel have given higher SFC, CO, HC and smoke density except NO_x in the marine engine (Karthikeyan et al. 2015). Effect of IT, EGR, IP on control of NO_x investigated fuelled with crude rice bran methyl ester based on DOE-Taguchi L9 orthogonal array after examination concluded that at no load and part load EGR is the most influencing factor. Still, at full load, IT is the most influencing factor in the control of NO_x. Based on the Signal to noise ratio for NO_x, BTE, and smoke density, the optimum condition at full load standard IT, 10% EGR, 240-250 bar IP. At no and part load, the optimum is standard IT, 10% EGR, 220-230 bar IP (De Serio, de Oliveira, and Sodr e 2017). Nano emulsive blends of GSB B5 are optimum at 23°bTDC to control NO_x and HC, and CO were reduced to 20.7% and 6.2% compared to diesel. Addition of EGR BSFC increases than the addition of nano emulsion GSB without EGR. Using a ternary blend of (70% diesel + 20% of waste low-density poly ethylene + 10% of 1-decanol) on a volume basis, performed experiments for output of ignition delay period, NO_x, HC, CO, and BTE at the engine's maximum power output by varying the CR and EGR, then found the optimum as 19:1 CR and 10% EGR as the better for ternary blends. Also, while increasing CR, ignition delay period, HC, CO, and smoke decreased except for BTE and NO_x (Shanmugam et al. 2021). Based on the RSM approach, the optimum condition is 13% GSB, 245bar IP, and 850 W EL for the output of BSFC, EGT, CO, HC, NO_x and smoke (USLU and YEŞİLYURT 2020). Sometimes nanoparticles are added as additives for enhancing performance and minimise emissions, and this enhancement effect depends on the type of base fuel chosen, the type of nanoparticle and their size (Venkatesan et al. 2017). RSM was used for analyzing CRDI engine performance and emission characteristics fuelled by linseed methyl ester at the fixed FIT of 23°bTDC at a constant speed of 1500 rpm, a compression ratio of 18 by varying influencing parameter of fuel blend, EGR, load, FIP and revealed the optimum combination at 5.45% of linseed methyl ester, 57.78MPa of FIP, 6.505% of EGR, 6.909kg of load (M. Kumar et al. 2022). (N. et al. 2021) Simarouba methyl ester was used in Kirloskar single cylinder direct injection diesel engine by varying load, FIP, nozzle hole, and orifice diameter and concluded that the increase in performance was seen by raise of FIP, increasing injector holes, and reducing the orifice diameter then the optimum variables found were 6 number of the hole, 240 bar of FIP, 0.2mm of hole

diameter. 20% mahua methyl ester in CRDI engine by varying FIP at 200, 400, 600bar and the FIT at 15, 20, 25-degree bTDC investigated and concluded that 800bar, 15 degree before top dead center as an optimum condition for better performance (P. Kumar et al. 2019). Emissions of a medium-duty engine were investigated by varying speed and load. The comparative analysis between rape seed biodiesel and animal raw fat pork lard-derived fuel were compared and concluded that bio-component rich concentration-based biodiesel optimization is required. Animal fat-derived fuels are superior to Rape seed-based biodiesel (DUDA et al. 2021). Varying EGR investigates 20% tallow biodiesel blend, FIP, FIT, load in CRDI engine then reported that 25% EGR, 600bar FIP, and 20°bTDC gave a better-expected performance (Kanthasamy, Selvan, and Shanmugam 2020). (S. Kumar and Dinesha 2018) RSM was used for the optimization of engine influencing parameters fuelled by Honge methyl ester by adjusting blend, engine load, IT, and compression ratio, then revealed the optimum condition such as 86.3% load, 15% of honge methyl ester, a compression ratio of 16, IT of 26.24°bTDC. Optimum combination for 17.5 compression ratio Kirloskar engine at 1500 rpm operation with nicotianatabaccum biodiesel were 45% of engine load, 30% of biodiesel blends, 240bar injection pressure, 30 degree before TDC (Sharma, Singh, Kumar Singh, et al. 2020). (Teoh et al. 2021) Found the optimum combination for moringa biodiesel 50% at 17.7 compression ratio by varying FIT from 3.625 to 10.38-degree bTDC, FIP from 264 to 936bar such as injection timing at 5-degree bTDC, 400 bar injection pressure. The optimum combination for neat lemon grass oil blended with diesel at 25% were 250 bar injection pressure, 26 degree before TDC, and 8.12 percent of EGR (Ramalingam et al. 2022). DOE-box Behnken RSM-based optimization in CRDI engine by using diesel as fuel is 20Nm EL, 750 bar IP, 12.5°bTDC, and also retarded IT leads to peak pressure shifted towards expansion stroke. The load has 56, 67, and 59% influence on NO_x, CO, and HC, respectively, 95% of mechanical efficiency effect influenced by IP and the IT has 73% influence on BSFC and load has 99% influence on BP, BMEP (Ramachander et al. 2021). Engine emission mainly depends on the start of the main injection followed by IP, and performance attributes especially depend on IP and % of injection quantity (Dond and Gulhane 2021). An increase of EL leads to shortened ignition delay at all fuel IT. Also, for B30, high-density poly ethylene oil with retarded IT and low EGR rates are best to control NO_x (Kulandaivel et al. 2020). In Argemone biodiesel of B20, the rise of pressure reduced the ignition delay and premixed heat release phase (M. Singh and Sandhu 2021). Various optimisation technique and diesel engine efficiency characteristics using various fuel and additives

are revealed (Abbas and Khan 2023; Faiz et al. 2024; Sivaram et al. 2020; Arul Peter et al. 2020; P Prakash and Dhanasekaran 2022; Paramasivam Prakash and Dhanasekaran 2023) (Sivaram et al. 2020; Arul Peter et al. 2020; P Prakash and Dhanasekaran 2022; Paramasivam Prakash and Dhanasekaran 2023)

The CRDI engine has gained widespread adoption in the automotive industry due to its remarkable efficiency and low emissions. Traditionally, these engines are optimized for conventional diesel fuel. However, the growing need for sustainable energy solutions has spurred interest in alternative fuels, such as biodiesel. Biodiesel offers numerous advantages, including reduced dependency on foreign oil, lower emissions of harmful pollutants and greenhouse gases, and potentially enhanced engine efficiency due to its higher oxygen content.

Despite these benefits, research on the performance of CRDI engines using Grape biodiesel is relatively sparse. The optimization of engine parameters for biodiesel-fueled CRDI engines is critical for realizing substantial improvements in both engine performance and emissions. Various factors-including operating environmental conditions, engine design and size, type of fuel used, and other parameters-affect the output responses of CRDI engines. Standard diesel engine settings are typically optimized for diesel fuel and may not be suitable for other fuel blends, such as those containing biodiesel. Given that the physical and chemical properties of biodiesel vary depending on the feedstock, it is essential to optimize engine parameters specifically for Grape biodiesel blends to achieve efficient performance and low emissions.

This study focuses on the optimization of engine parameters using a desirability-based RSM approach, specifically examining diesel blended with various proportions of grape biodiesel. The input parameters considered for optimization include engine load, fuel blend, fuel IP, IT, and EGR. The output performance parameters considered are BMEP, BTE, SFC, mechanical efficiency, and emissions of CO, NO_x, and HC.

The novelty of this research lies in its comprehensive and systematic approach to optimizing the combustion of grape seed biodiesel in a CRDI diesel engine. Unlike conventional studies that focus on more common biodiesel sources and direct injection engines, this study investigates the less commonly explored grape seed biodiesel, providing new insights into its unique combustion characteristics. These characteristics include higher viscosity, different energy content, and distinct

emission profiles, especially at high injection pressures up to 1000 bar. By utilizing a sophisticated multi-parameter optimization framework, the study employs a CCD matrix and RSM to fine-tune key engine parameters such as injection timing, injection pressure, engine load, and EGR. Modern ECU technology allows for precise adjustments, enhancing both engine performance and emission reductions.

Through testing fifty input combinations, the study systematically identifies the optimal settings, recommending specific parameters: 6° bTDC injection timing, 82% engine load, 6.7% EGR, 1000 bar injection pressure, and a 33% biodiesel blend. This rigorous approach ensures a balanced improvement in BTE, BMEP, and mechanical efficiency, while reducing SFC, HC, NO_x, and CO emissions. Consequently, this research significantly advances the practical application and understanding of grape seed biodiesel in CRDI engines, offering valuable contributions to the field of alternative fuels.

Materials

The raw seed oil was converted into biodiesel by a general transesterification process for removing the gummy content, glycerol and to reduce the viscosity of the test fuel. Prepared biodiesel properties like acid value, specific gravity, density, calorific value, viscosity and flash point was analyzed by following ASTM standard and the comparison with base fuel is shown in table 1. Approximately all the properties are nearer to diesel fuel is a good sign for use as an alternative fuel. The Flash and fire point of the grape seed biodiesel is higher than the reference fuel; hence there is no storage issue with the biodiesel. The calorific value of pure grape seed biodiesel is lower, and the density of biodiesel is higher than base fuel, so blending is necessary to avoid excessive fuel consumption and achieve better performance and emissions.

Table 1: Properties of Grape Biodiesel

| Properties | Unit | Standard Diesel | Grape seed Biodiesel | ASTM Standard |
|------------------|---------------------|-----------------|----------------------|---------------|
| Acid Value | mg of KOH/gm of oil | 0.6 | 0.48 | D6751 |
| Free Fatty Acid | % | 0.3 | 0.24 | -- |
| Specific Gravity | -- | 0.816 | 0.869 | D287 |
| Density | kg/m ³ | 816 | 869 | D287 |

| | | | | |
|--------------------------------|------------|--------|------|----------|
| Lower Calorific Value | calorie/gm | 10,236 | 8712 | D 4809 |
| Higher Calorific Value | calorie/gm | 10,822 | 9298 | D 4809 |
| Flash Point | °C | 53 | 95 | D 93-58T |
| Fire Point | °C | 56 | 100 | D 93-58T |
| Kinematic viscosity @ 40° C | CSt | 2.09 | 3.62 | D445 |
| Dynamic viscosity at 40° C | cP | 1.73 | 3.15 | D445 |



Figure 1a: grape seed biodiesel blends

Experimental setup and procedure

The device used for experimental work is shown in figure 1. The practical work was conducted under atmospheric conditions by modifying the engine's input such as injection pressure, injection timing, engine load, fuel blend, and EGR at a fixed speed of 1500 rpm and a compression ratio of 18 according to the design matrix developed in RSM by the high accurate central composite method. By altering the influencing parameter, there were fifty observations, and the data were analyzed by IC engine software developed by the apex. Design expert software was used to model design of experiment by following efficient central composite design method shown in table 12,

Random order-based experimental work was conducted and recorded the outcome. Specifications and accuracy of experimental setup have shown in table 2, 3 and 4. Five parameter and five level used for CCD based DOE is shown in table 5.



Figure 1: photograph of Experimental setup

Table 2: Instrumental Accuracy

| Name of device/Instrument | Company/Model | Used for | Accuracy |
|----------------------------------|--------------------------------|--------------------------------------|-----------------|
| Pressure sensor | PCB Pizotronics USA/M111A22 | In cylinder Pressure | -0.01 |
| Analog Temperature Transmitter | WIKA, Pune | Water and exhaust gas temperature | 0.50% |

| | | | |
|-----------------------------------|------------------------------|----------------------|--------------------------|
| Speed Indicator | Selectron, Mumbai | RPM indicator | 0.05% |
| Encoder | Kubler Germany | Crank angle and RPM | 0.25% |
| Load cell | Sensortronics, Chennai/60001 | Measure load | 0.25% F.S. (0.125 kg) |
| Load Indicator | ABUS Technologies Inc. | Display applied load | 0.2% F.S |
| Differential Pressure Transmitter | Yokogawa/EJA110A-DMS5A-92NN | Flow rate of fuel | 0.10% |
| Pressure Transmitter | Wika instruments, SL1, Pune | Flow rate of air | 0.50% |
| Rotameter | PG-1 to 21 Eureka Pune | Flow rate of water | 2% F.S. |

Table 3: specifications of experimental setup

| Engine Components | Specifications |
|--------------------|---|
| Make | Kirloskar |
| Type | CRDI VCR engine, single chamber, 4 stroke, water cooling type, CR (12-18) |
| Dimensions | Swept length 110 mm, cylinder dia 87.5 mm, swept volume 661.5 cm ³ . |
| Combustion chamber | Hemispherical bowl, connecting rod length 234 mm |
| Power | 3.5 KW @1500 rpm |
| Compression ratio | 18 |
| Load | Eddy current dynamometer type, arm length 185 mm |
| EGR type | water cooled |
| ECU Model | Nira i7r |
| Piezo sensor | Combustion range 350 bar with low noise cable |
| Crank angle sensor | Resolution 1 Deg, Speed 5500 RPM with TDC pulse |
| Data acquisition | NI USB-6210, 16-bit, 250ks/s |
| Temperature Sensor | RTD Type, PT100, Type K |

| | |
|-------------------------|--|
| Load sensor | strain gauge type type, 0-50 Kg |
| Nozzle | 7 Hole & diameter 250 micrometer |
| Rotameter | Engine cooling 40-400 LPH, Calorimeter 25-250 LPH |
| Temperature Transmitter | type 2 wire, Input RTD PT 100, Range 0-100 deg C, output 4-20 mA |
| Setup overall dimension | W2000 X D2500 X H1500 |

Table 4: range and resolution of exhaust gas analyzer

| Parameters | Measurement | Resolution |
|-----------------|----------------------|-------------------------------------|
| CO | 0 ... 15 % Vol. | 0.001% Vol. |
| HC | 0 ... 20000 ppm Vol. | 1 ppm/10 ppm (0-2000ppm)/(>2000ppm) |
| NO | 0 ... 5000 ppm Vol. | 1 ppm Vol. |
| Engine speed | 400 ... 6000 rpm | 1 rpm |
| Oil temperature | 0 -125 deg. C | 1 deg. C |
| Lambda | 0 ... 9.999 | 0.001 |

Table 5: Influencing parameter level for DOE

| Name | Units | Factor | Levels | | | | |
|------|-------|--------|--------|-----|-----|-----|------|
| | | | -2 | -1 | 0 | 1 | 2 |
| FB | % | A | 0 | 15 | 30 | 45 | 60 |
| EL | % | B | 20 | 40 | 60 | 80 | 100 |
| IP | Bar | C | 400 | 550 | 700 | 850 | 1000 |
| IT | bTDC | D | 6 | 12 | 18 | 24 | 30 |
| EGR | % | E | 0 | 4 | 8 | 12 | 16 |

Table 6: Summary of developed model

| Response | Source | SS | df | MS | F-value | p-value |
|----------|-------------|--------|----|--------|---------|----------|
| SFC | Model | 0.1801 | 20 | 0.009 | 5.57 | < 0.0001 |
| | Lack of Fit | 0.0274 | 22 | 0.0012 | 0.4476 | 0.9293 |
| BMEP | Model | 29.05 | 20 | 1.45 | 2770.65 | < 0.0001 |
| | Lack of Fit | 0.0108 | 22 | 0.0005 | 0.7843 | 0.6925 |

| | | | | | | |
|-------|-------------|----------|----|----------|--------|----------|
| BTHE | Model | 0.0003 | 20 | 0 | 5.14 | < 0.0001 |
| | Lack of Fit | 0.0001 | 22 | 2.38E-06 | 0.4025 | 0.9515 |
| MECH | Model | 4398.79 | 20 | 219.94 | 84.86 | < 0.0001 |
| EFFI. | Lack of Fit | 66.26 | 22 | 3.01 | 2.37 | 0.1222 |
| CO | Model | 0.3393 | 20 | 0.017 | 23.38 | < 0.0001 |
| | Lack of Fit | 0.0192 | 22 | 0.0009 | 3.3 | 0.0551 |
| HC | Model | 402.59 | 20 | 20.13 | 3.68 | 0.0007 |
| | Lack of Fit | 120.69 | 22 | 5.49 | 1.01 | 0.536 |
| NO | Model | 4.20E+06 | 20 | 2.10E+05 | 14.66 | < 0.0001 |
| | Lack of Fit | 3.13E+05 | 22 | 14203.48 | 0.9644 | 0.5655 |

Table 7: ANOVA of Responses

| | Source | Model | A-FB | B-EL | C-IP | D-IT | E-EGR | A ² | B ² | C ² | D ² | E ² | Interaction |
|------|---------|---------|--------|----------|--------|--------|--------|----------------|----------------|----------------|----------------|----------------|-------------|
| SFC | F value | 5.57 | 0.8178 | 67.53 | 5.75 | 13.95 | 0.0139 | | | * | * | | |
| | p value | 0.0001 | 0.3733 | 0.0001 | 0.0231 | 0.0008 | 0.9069 | | | | | | |
| | F value | 2770.65 | 0.4769 | 55390.65 | 0.9347 | 0.0191 | 0.9347 | | | * | | * | |
| BMEP | F value | 0.0001 | 0.4953 | 0.0001 | 0.3416 | 0.8911 | 0.3416 | | | | | | |
| | p value | 1 | 53 | 6 | 1 | 6 | | | | | | | |
| | F value | 5.14 | 0.325 | 63.38 | 6.07 | 12.2 | 0.1766 | | | * | * | | |
| BTHE | p value | 0.0001 | 0.573 | 0.0001 | 0.0199 | 0.0016 | 0.6774 | | | | | | |
| | F value | 84.86 | 0.7589 | 1624.79 | 0.2598 | 32.66 | 0.2781 | | | | | | |
| | p value | 0.0001 | 0.3908 | 0.0001 | 0.6141 | 0.0001 | 0.6019 | | | * | | | DE |

| | | | | | | | | | |
|-----|---------|--------|--------|--------|--------|--------|--------|---|------------|
| CO | F value | 23.38 | 4.33 | 341.06 | 0.2358 | 7.13 | 37.48 | * | AE, BE, CD |
| | p value | 0.0001 | 0.0465 | 0.0001 | 0.6309 | 0.0123 | 0.0001 | | |
| HC | F value | 3.68 | 5.6 | 6.25 | 0.2239 | 11.88 | 10.97 | * | * AE,CD |
| | p value | 0.0007 | 0.0249 | 0.0183 | 0.6396 | 0.0018 | 0.0025 | | |
| NOx | F value | 14.66 | 0.9631 | 3.89 | 2.14 | 61.45 | 193.26 | * | * BE, DE |
| | p value | 0.0001 | 0.3345 | 0.0582 | 0.1544 | 0.0001 | 0.0001 | | |

*- significant

Table 8: Predicted Fit statistics

| Components | SFC | BMEP | BTHE | MECH EFFI. | CO | HC | NO |
|--------------------------|---------|----------|---------|---------------|---------|--------|---------|
| R ² | 0.79 | 0.9995 | 0.7799 | 0.9832 | 0.9416 | 0.7173 | 0.91 |
| Adjusted R ² | 0.6509 | 0.9991 | 0.628 | 0.9716 | 0.9013 | 0.5223 | 0.8479 |
| Predicted R ² | 0.4171 | 0.9984 | 0.3908 | 0.9432 | 0.7856 | 0.0783 | 0.7186 |
| Adeq Precision | 11.7029 | 229.6802 | 11.1866 | 39.3372 | 20.1354 | 8.3114 | 16.7612 |

Performance and Emission characteristics

The CRDI engine was operated based on the design matrix, and their RSM 3-dimensional surface graphs are discussed below. Fuel blend, engine load, injection pressure, injection timing, and exhaust gas recirculation are the considered input parameters. The response surface graphs are plotted by viewing the two input parameters while maintaining the remaining three input parameters at the mid-level of the ranges, as shown in figures 2 to 29. Summary of developed model, ANOVA and fit statistics are shown in table 6, 7 and 8. For the entire developed model p-value is less than 0.0001.

Mechanical Efficiency (%)

Design Points:

● Above Surface

○ Below Surface

25.98  68.87

X1 = A

X2 = B

Actual Factors

C = 700

D = 18

E = 8

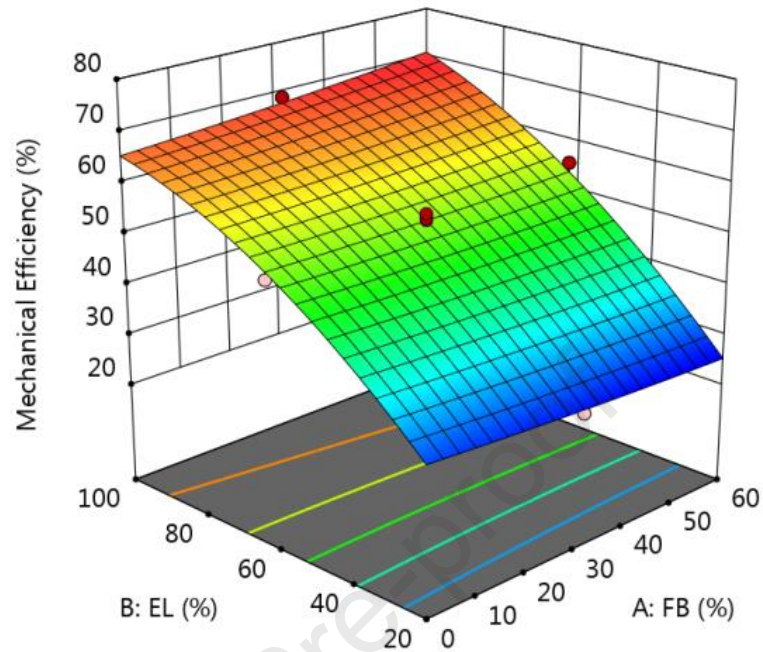


Figure: 2 EL vs FB effect on Mechanical efficiency

The interaction effect of biodiesel mixed with diesel blends and engine load on mechanical efficiency is shown in figure 2. At maximum load of CRDI engine operation, there was a significant increase in mechanical efficiency with the increase of biodiesel blend in diesel as fuel due to lubricant effect caused by blended fuel. The maximum and minimum mechanical efficiency during experimental work were 25.98 to 68.87%.

Mechanical Efficiency (%)

Design Points:

● Above Surface

○ Below Surface

25.98  68.87

X1 = B

X2 = C

Actual Factors

A = 30

D = 18

E = 8

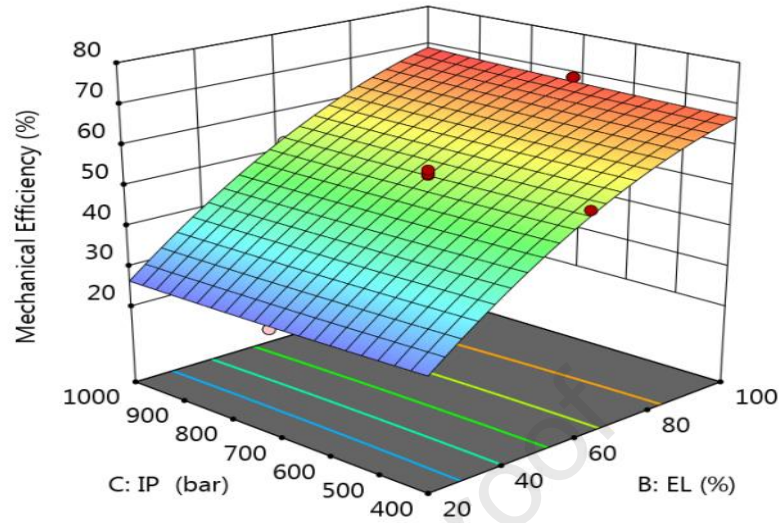


Figure: 3 Effect of IP, EL on Mechanical efficiency

There is a slight increase in the mechanical efficiency of the CRDI engine with the rise of fuel injection pressure towards the maximum of 1000bar pressure from 400bar at full load, shown in figure 3. By comparing EL and IP, the EL is the main influencing effect on mechanical efficiency.

$$\begin{aligned} \text{Mechanical Efficiency} = & 18.3979 + -0.160608 * \text{FB} + 0.808128 * \text{EL} + -0.00315417 * \text{IP} + - \\ & 0.226406 * \text{IT} + -0.61801 * \text{EGR} + 0.00188021 * (\text{FB} * \text{EL}) + 4.125\text{e-}05 * (\text{FB} * \text{IP}) + 0.00133681 \\ & * (\text{FB} * \text{IT}) + -0.00188021 * (\text{FB} * \text{EGR}) + 7.09375\text{e-}05 * (\text{EL} * \text{IP}) + 0.000888021 * (\text{EL} * \text{IT}) + \\ & 0.000542969 * (\text{EL} * \text{EGR}) + -0.000409375 * (\text{IP} * \text{IT}) + 0.000230729 * (\text{IP} * \text{EGR}) + 0.0236849 * \\ & (\text{IT} * \text{EGR}) + 0.000411389 * \text{FB}^2 + -0.00351234 * \text{EL}^2 + 2.89167\text{e-}06 * \text{IP}^2 + 0.0131267 * \\ & \text{IT}^2 + 0.00547266 * \text{EGR}^2 \end{aligned}$$

Mechanical Efficiency (%)

Design Points:

● Above Surface

○ Below Surface

25.98  68.87

X1 = B

X2 = D

Actual Factors

A = 30

C = 700

E = 8

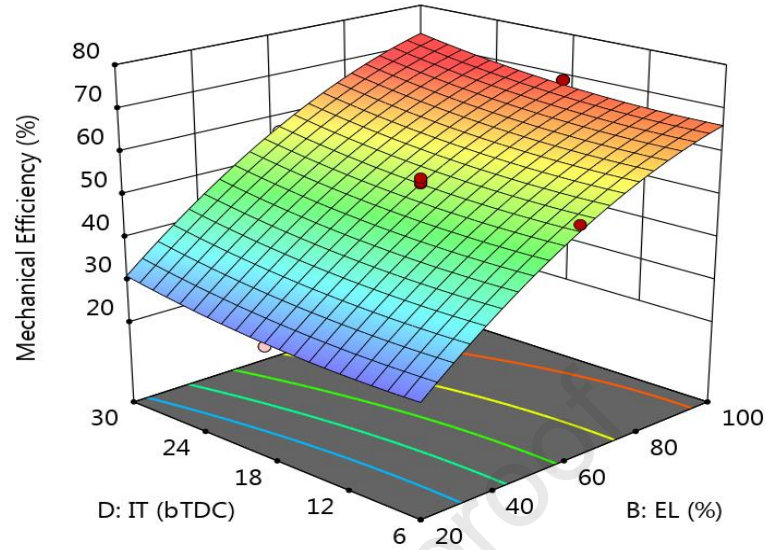


Figure 4: Effect of IT, EL on Mechanical efficiency

Advancing injection timing too away from top dead center there is a considerable increase in the mechanical efficiency of CRDI engine than injecting fuel nearer to TDC at a full load of engine operations due to better lubrication is shown in figure 4.

Mechanical Efficiency (%)

Design Points:

● Above Surface

○ Below Surface

25.98  68.87

X1 = D

X2 = E

Actual Factors

A = 30

B = 60

C = 700

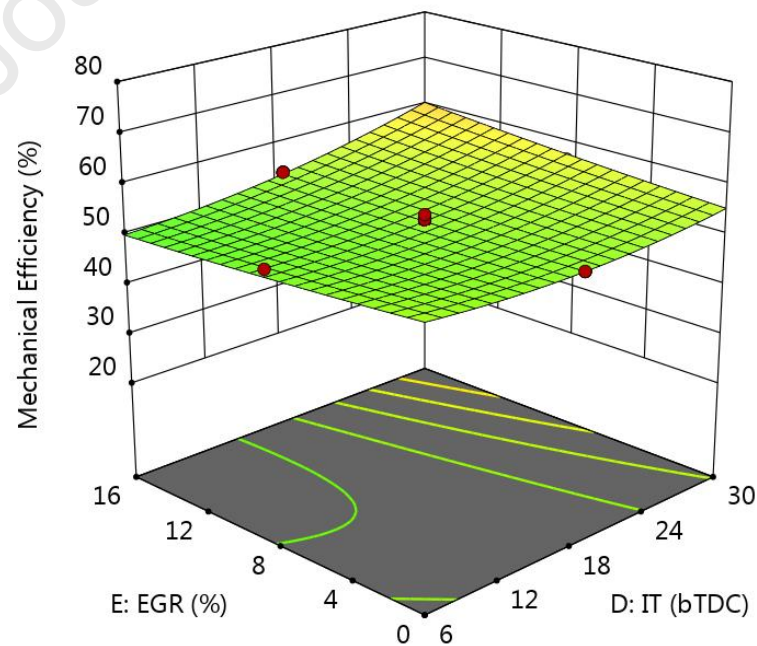


Figure 5: Effect of EGR, IT on mechanical efficiency

Advancing injection timing from 6 to 30 degrees before top dead center and increasing the EGR rate from zero to 16 percent turns into increased mechanical efficiency, as shown in figure 5. From figure 5, it is clear that the maximum mechanical efficiency was observed at 30 degrees before TDC and 16% of EGR. EGR effect on mechanical efficiency at injection timing near TDC gives less variation than advancing away from the TDC effect.

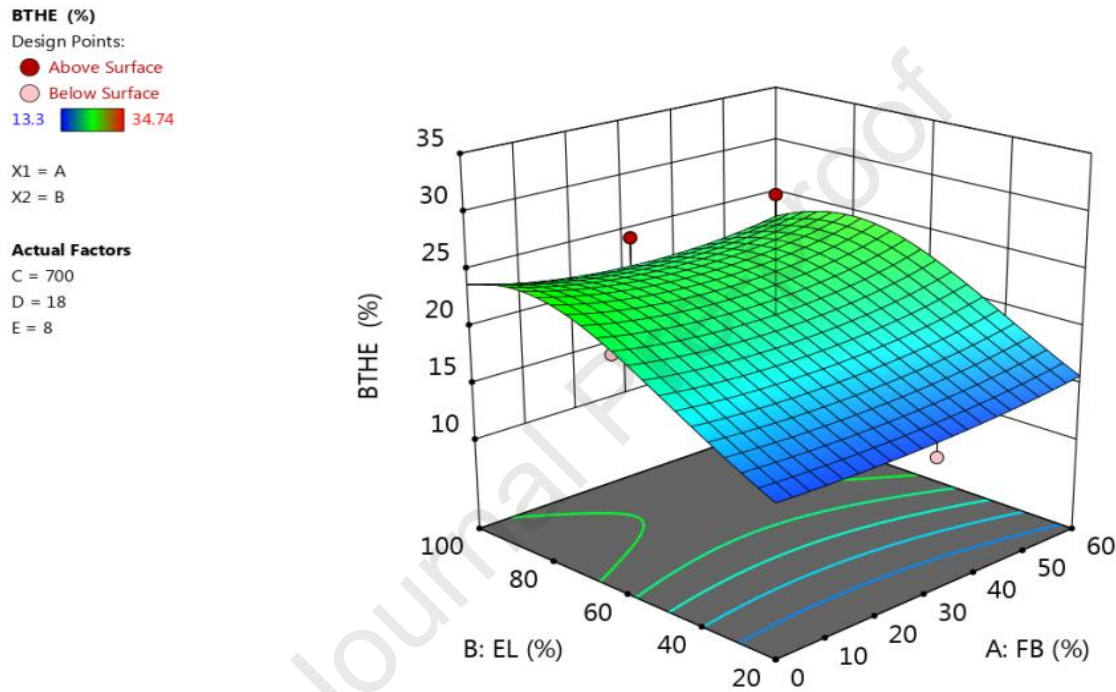


Figure 6: effect of EL, FB on BTHE

The response variation of engine load versus fuel blend is shown in figure 6. Maximum BTE was seen when operating the engine at around 80 to 85% engine load and petroleum diesel as fuel. An increasing trend of BTE was seen when increasing engine load for all the fuels used for analysis, but thermal efficiency decreased for every test fuel beyond 85% of engine load. Figure 6 shows that BTHE variation for B0, B15, B30, B45, and B60% is less than engine load. The maximum and minimum BTE observed during experimental work were 13.3 to 27.04 percent.

Factor Coding: Actual

BTE (%)

Design Points:

● Above Surface

○ Below Surface

13.3  27.04

X1 = B

X2 = C

Actual Factors

A = 30

D = 18

E = 8

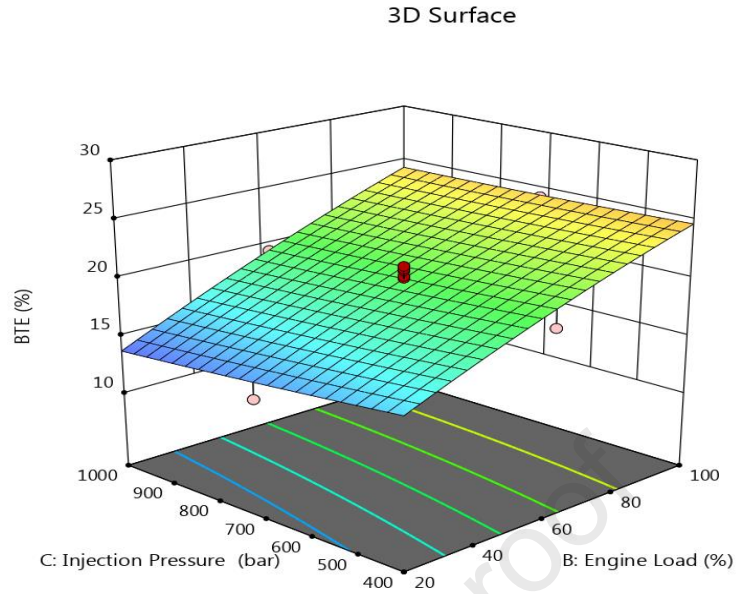


Figure 7: effect of IP, EL on BTHE

IP versus EL on BTHE is shown in figure 7. Maximum BTE was seen at a lower injection pressure of 400bar and 100% engine load. When injection pressure increased, there was no considerable change in BTHE. Even the 1000bar function reported BTE is slightly less than 400bar of process.

$$\begin{aligned} (\text{BTE})^{-1.44} = & 0.00613328 + 2.16357\text{e-}05 * \text{FB} + -0.000388959 * \text{EL} + 5.41489\text{e-}05 * \text{IP} + \\ & 0.00011785 * \text{IT} + -0.000426754 * \text{EGR} + 5.62696\text{e-}07 * (\text{FB} * \text{EL}) + -7.35464\text{e-}08 * (\text{FB} * \text{IP}) + \\ & 3.19594\text{e-}06 * (\text{FB} * \text{IT}) + 6.27071\text{e-}07 * (\text{FB} * \text{EGR}) + -7.14331\text{e-}08 * (\text{EL} * \text{IP}) + -1.98234\text{e-}06 * \\ & (\text{EL} * \text{IT}) + 4.15004\text{e-}06 * (\text{EL} * \text{EGR}) + 8.83715\text{e-}08 * (\text{IP} * \text{IT}) + 1.62689\text{e-}07 * (\text{IP} * \text{EGR}) + - \\ & 9.4547\text{e-}07 * (\text{IT} * \text{EGR}) + -1.2876\text{e-}06 * \text{FB}^2 + 2.59567\text{e-}06 * \text{EL}^2 + -3.27739\text{e-}08 * \text{IP}^2 + \\ & 4.53311\text{e-}07 * \text{IT}^2 + 2.01443\text{e-}06 * \text{EGR}^2 \end{aligned}$$

BTHE (%)

Design Points:

● Above Surface

○ Below Surface

13.3  34.74

X1 = B

X2 = D

Actual Factors

A = 30

C = 700

E = 8

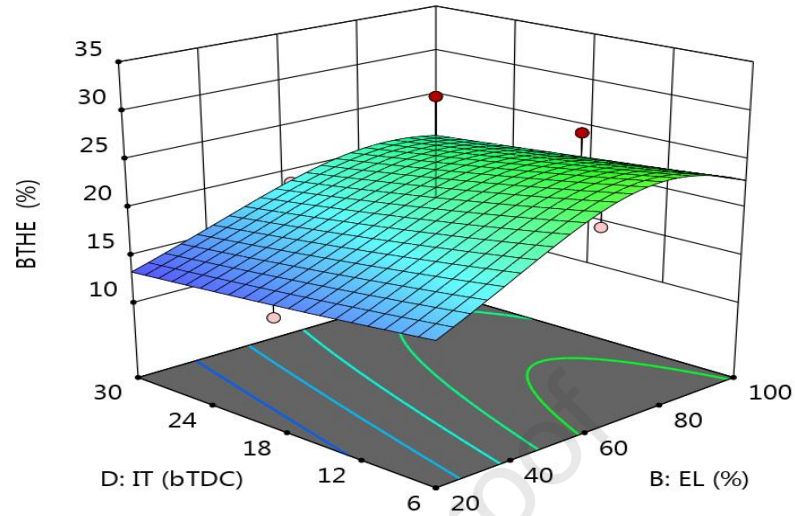


Figure 8: effect of IT, EL on BTHE

IT versus EL on BTE is shown in figure 8. An increase in BTE with a rise in engine load is further increased when injecting fuel nearer to TDC than injecting too far away from the top dead center. For all the engine load operations, BTHE was slightly less when injecting fuel at 30 degrees before TDC than 6 degrees before TDC. Injection timing variation on BTHE is very minimum to the engine load effect. An ignition delay is less due to high temperature and pressure leading to considerable increase in BTHE when the fuel is injected near the TDC than advanced injection,

BTHE (%)

Design Points:

● Above Surface

○ Below Surface

13.3  34.74

X1 = B

X2 = E

Actual Factors

A = 30

C = 700

D = 18

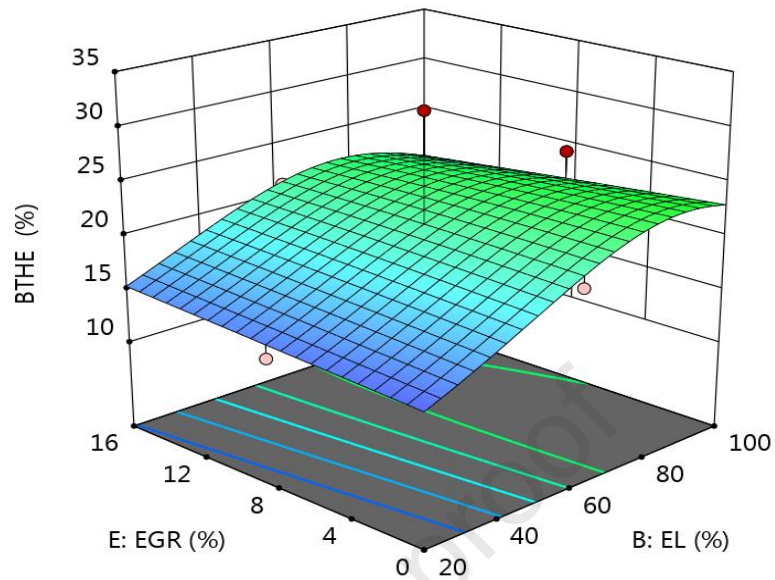


Figure 9: Effect of EGR, EL on BTHE

EGR versus EL on BTHE is shown in figure 9. Adding EGR reduces the increase in BTE with a rise in load. Maximum BTE was observed at around 80% engine load and without the addition of EGR. The addition of EGR at low load and moderate load has not much effect on BTE, but the addition of EGR at high load has a greater effect on BTE; that is the addition of EGR at full load leads to a reduction of BTE due to lack of oxygen, energy density, and combustion temperature.

BMEP (bar)

Design Points:

● Above Surface

○ Below Surface

0.89  4.24

X1 = A

X2 = B

Actual Factors

C = 700

D = 18

E = 8

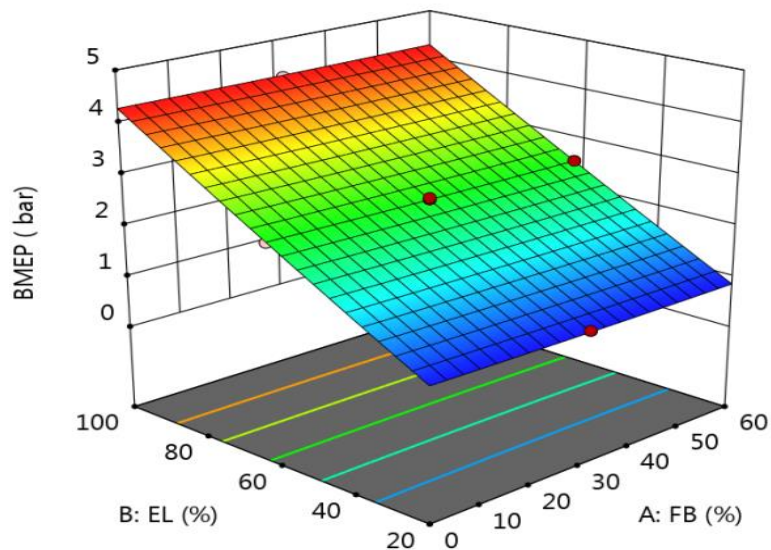


Figure 10: effect of EL, FB on BMEP

The interactive effect of EL versus FB on BMEP is shown in figure 10. From the graph, it is clear that BMEP depends mainly on engine load than on other responses considered for the analysis. There is an increasing trend of BMEP when increasing engine load and no change in direction for all the test samples. BMEP has linear relationship with engine load.

$$\begin{aligned} \text{BMEP} = & 0.1781 + -0.00157778 * \text{FB} + 0.0407208 * \text{EL} + -0.000193333 * \text{IP} + -0.00606944 * \text{D} \\ & + 0.0039375 * \text{EGR} + 8.33333\text{e-}06 * (\text{FB} * \text{EL}) + 1.11111\text{e-}06 * (\text{FB} * \text{IP}) + -2.77778\text{e-}05 * (\text{FB} * \text{IT}) \\ & + -2.08333\text{e-}05 * (\text{FB} * \text{EGR}) + 4.16667\text{e-}07 * (\text{EL} * \text{IP}) + -5.20833\text{e-}05 * (\text{EL} * \text{IT}) + -6.25\text{e-}05 * \\ & (\text{EL} * \text{EGR}) + -1.38889\text{e-}06 * (\text{IP} * \text{IT}) + -6.25\text{e-}06 * (\text{IP} * \text{EGR}) + 5.20833\text{e-}05 * (\text{IT} * \text{EGR}) + \\ & 1.33333\text{e-}05 * \text{A}^2 + 2.3125\text{e-}05 * \text{EL}^2 + 1.33333\text{e-}07 * \text{IP}^2 + 0.000291667 * \text{IT}^2 + 0.0001875 \\ & * \text{EGR}^2 \end{aligned}$$

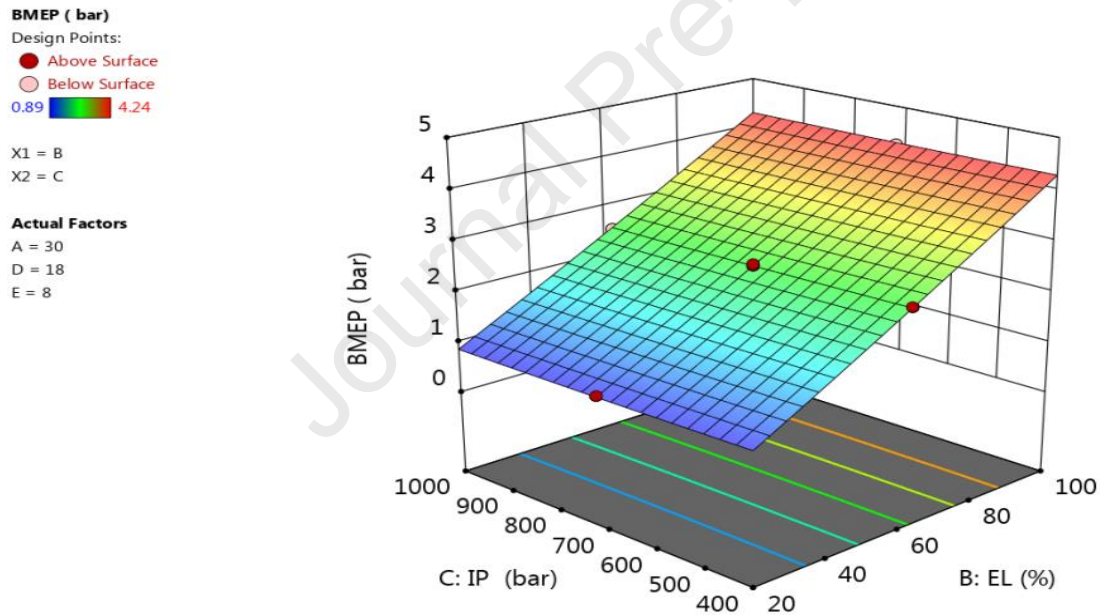


Figure 11: effect of IP, EL on BMEP

The interactive effect of IP versus EL on BMEP is shown in figure 11. For all the variations of IP from 400 bar to 1000 bar and increase of EL there was a gradual increase in BMEP reported. The effect of IP on BMEP is very less than engine load. During analysis, 0.89 to 4.24bar BMEP was seen as the highest and lowest levels

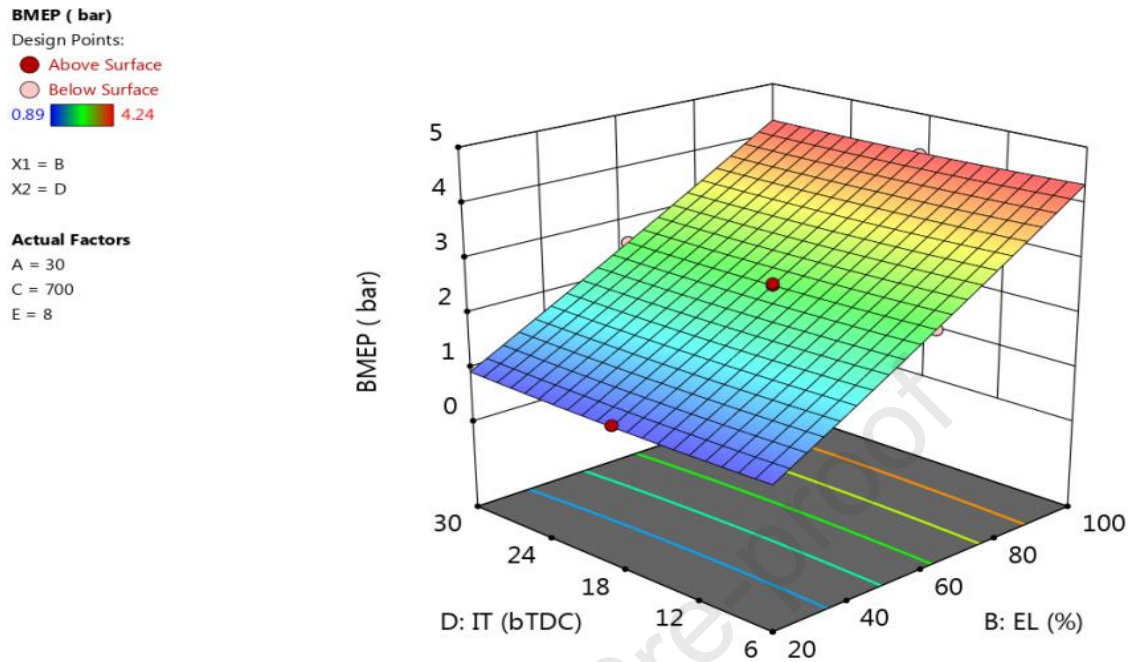


Figure 12: effect of IT, EL on BMEP

The interactive effect of EL versus IT on BMEP is shown in figure 12. From the graph, it is clear that variation of injection timing effect on BMEP is less influential than engine load. Engine load is the primary influencing parameter for the considered IT ranges and EL.

BMEP (bar)

Design Points:

● Above Surface

○ Below Surface

0.89  4.24

X1 = B

X2 = E

Actual Factors

A = 30

C = 700

D = 18

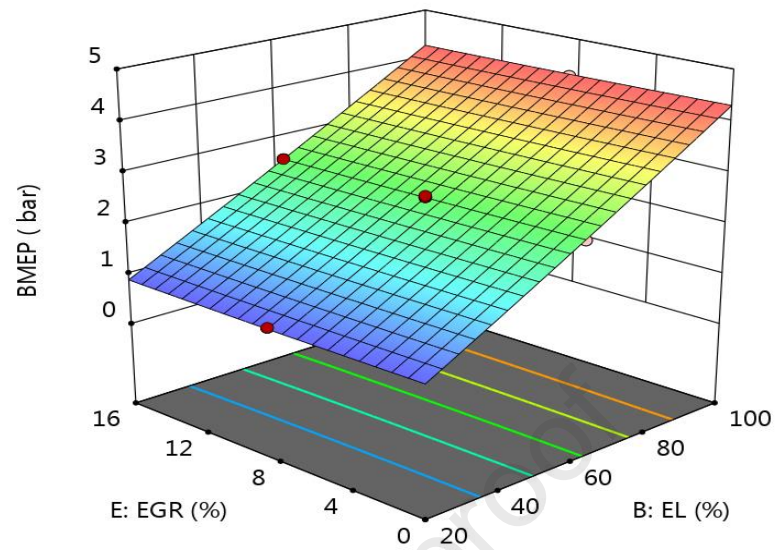


Figure 13: effect of EGR, EL on BMEP

EGR vs EL effect on BMEP is shown in figure 13. Adding EGR at various recirculation rates has no considerable impact on developed BMEP than as influenced by engine load. Engine load is the primary influencing parameter compared with EGR on BMEP.

CO (% vol)

Design Points:

● Above Surface

○ Below Surface

0.04  0.32

X1 = A

X2 = B

Actual Factors

C = 700

D = 18

E = 8

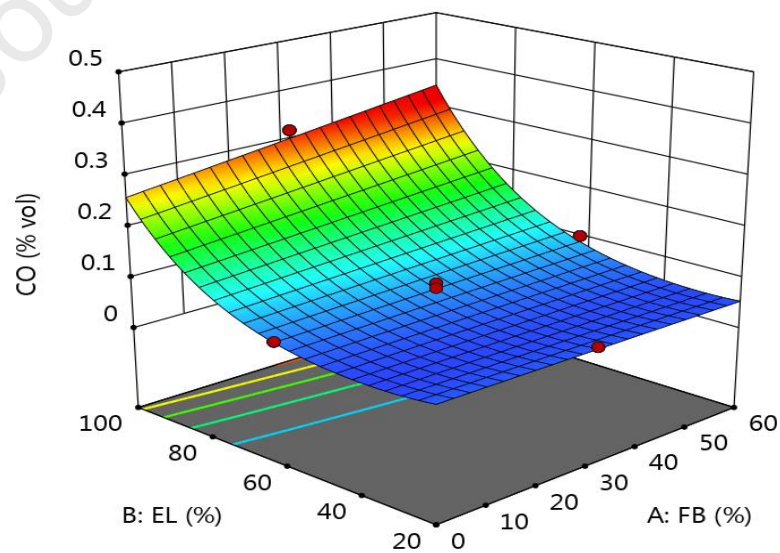


Figure 14: effect of EL, FB on CO

The interactive effect of EL versus FB on carbon monoxide is shown in figure 14. Maximum CO was reported at a higher percent blend of B60 and 100% of engine load. Increased CO and increased EL are significantly reduced by using petrodiesel as fuel than grape seed biodiesel blended with diesel blends. Beyond 80% of engine load, all test fuel samples saw a tremendous increase in CO. Still, and Unblended diesel fuel gave lower CO than blended grape seed biodiesel due to property variation from diesel fuel.

$$\begin{aligned} \text{Sqrt}(\text{CO}) = & 0.642498 + 0.000304169 * \text{FB} + -0.0067767 * \text{B} + -0.000606295 * \text{IP} + -0.0172857 \\ & * \text{IT} + 0.00943354 * \text{EGR} + 1.83016\text{e-}05 * (\text{FB} * \text{EL}) + 5.16172\text{e-}07 * (\text{FB} * \text{IP}) + 2.93841\text{e-}05 * \\ & (\text{FB} * \text{IT}) + -0.000203647 * (\text{FB} * \text{EGR}) + -1.07085\text{e-}06 * (\text{EL} * \text{IP}) + 1.97352\text{e-}05 * (\text{EL} * \text{IT}) + \\ & 0.000252238 * (\text{EL} * \text{EGR}) + 1.4536\text{e-}05 * (\text{IP} * \text{IT}) + -6.75546\text{e-}06 * (\text{IP} * \text{EGR}) + -0.000146631 * \\ & (\text{IT} * \text{EGR}) + -1.21149\text{e-}06 * \text{FB}^2 + 7.11409\text{e-}05 * \text{B}^2 + 3.09763\text{e-}07 * \text{IP}^2 + 0.00022537 * \\ & \text{IT}^2 + -0.00028573 * \text{EGR}^2 \end{aligned}$$

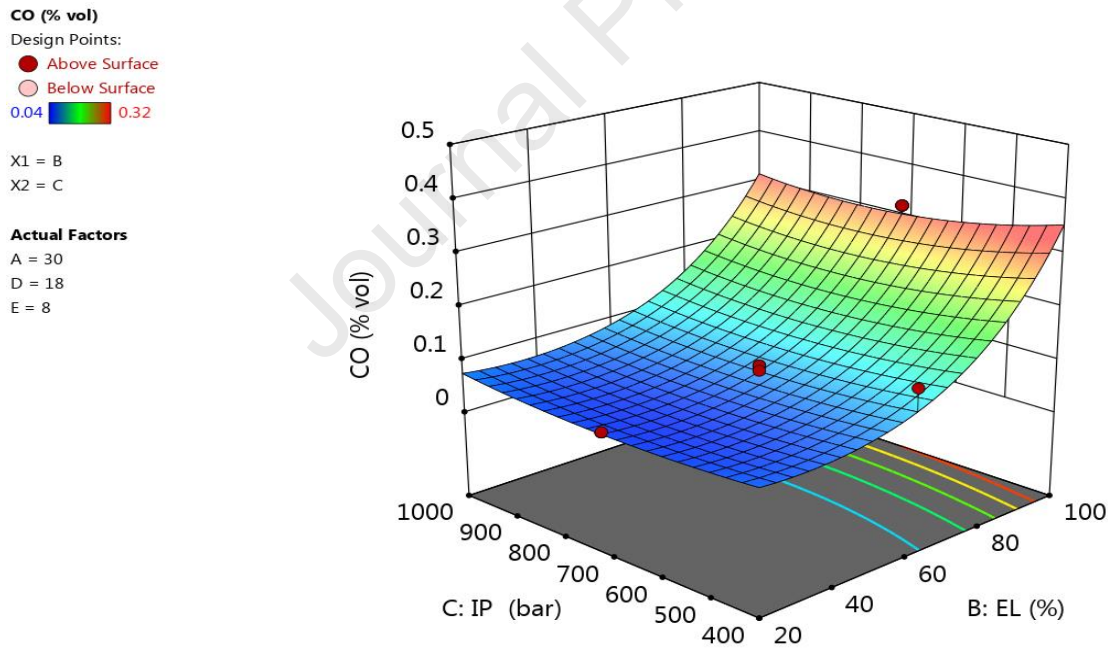


Figure 15: effect of IP, EL on CO

The interactive effect of IP versus EL on CO is shown in figure 15. Increased CO along with increased engine load is decreased by the variation of IP minimum 400 bar to a higher level of IP, but still, CO is high than the low load of operation. The maximum and minimum CO reported

during experimental work is 0.04 to 0.32% on volume-based. The ultimate CO was registered at a low injection pressure of 400 bar and a high engine load of 12.3 kg.

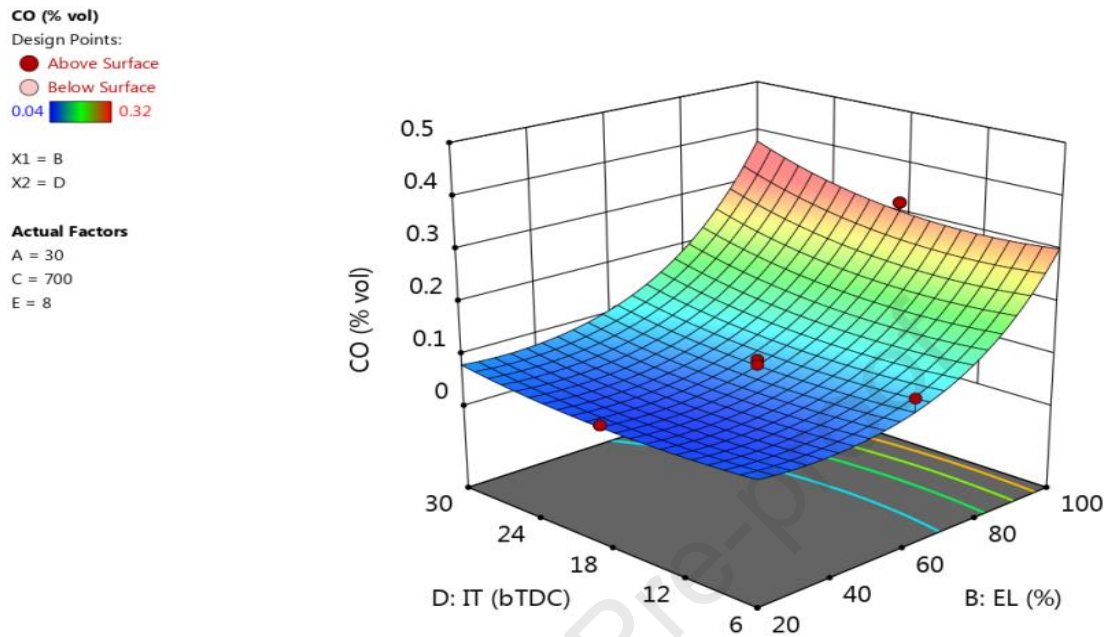


Figure 16: effect of IT, EL on CO

The interactive effect of injection timing versus engine load on CO is shown in figure 16. Increased CO and engine load increase are further increased by advancing fuel injection towards 30 degree from 6 degree before TDC. The maximum CO emission was reported at 30 degree bTDC and 100% of engine load. At partial load operation the variation of injection timing not cause greater effect than at above 65% of CRDI diesel engine load effect on CO. Also above 60% of engine load, CO formation due to injection time variation is very minimum than engine load effect.

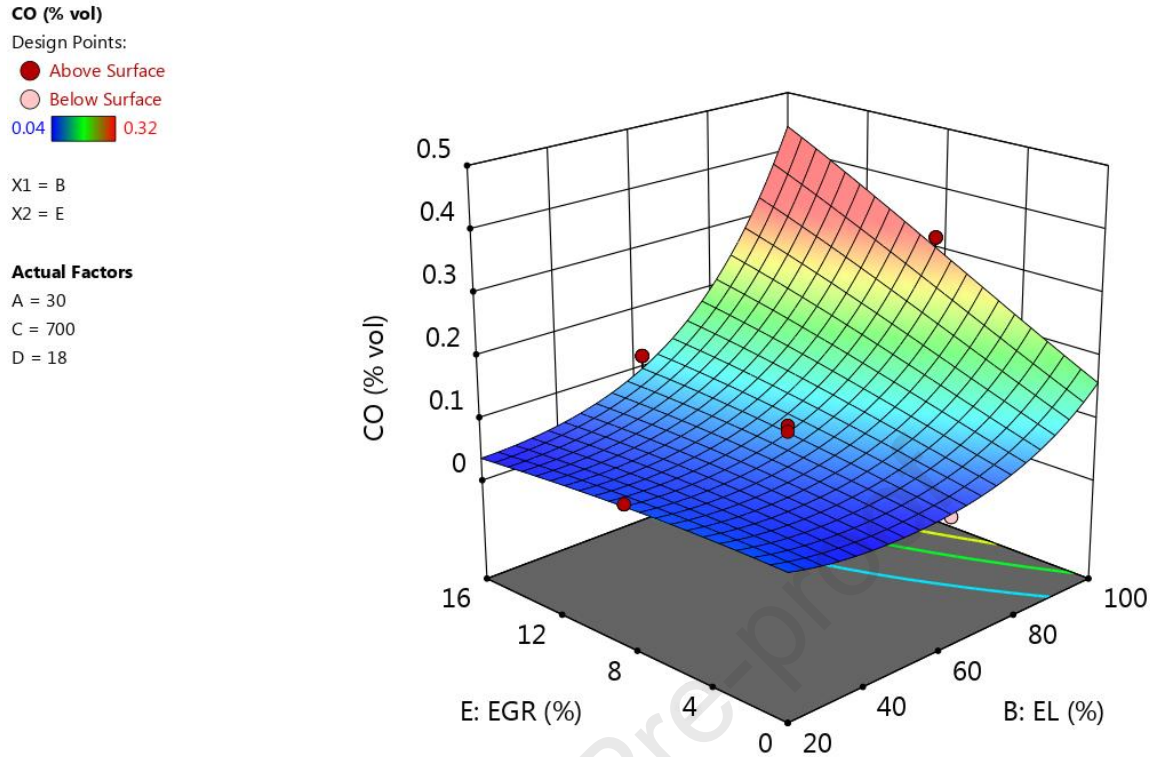


Figure 17: effect of EGR, EL on CO

The interactive effect of EGR vs EL on CO response is shown in figure 17. An increase in CO along with engine load is considerably further enhanced with the addition of EGR. The maximum carbon monoxide emission was seen at full engine load (12.3kg) and complete (16%) exhaust gas recirculation. The addition of EGR leads to the shortage of oxygen required for combustion turns into an enhancement in carbon monoxide emissions. At a full load of engine operation without exhaust gas recirculation gave lower CO, but still, it is higher than quiet load operation with EGR. The addition of EGR upto 60% of engine load does not affect CO formation more than that of EGR beyond 60% of engine load. At low load, there is no more significant CO formation variation than at full load due to EGR addition

HC (PPM vol)

Design Points:

● Above Surface

○ Below Surface

7  23

X1 = A

X2 = C

Actual Factors

B = 60

D = 18

E = 8

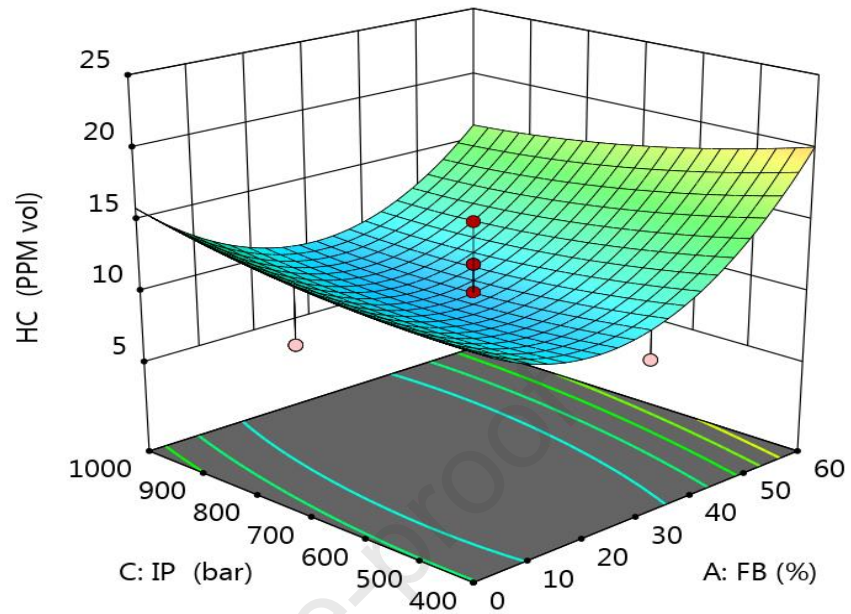


Figure 18: effect of IP, FB on HC

IP vs FB effect on hydrocarbon emission is shown in figure 18. At 60% of FB with the increase of injection pressure towards 1000bar turns into a reduction in HC emission. The maximum and minimum value of 7 and 23ppm of HC was observed during experimentation. The lowest HC was reported when the engine was operated at approximately 25% biodiesel blend for various IPs considered for the investigations. There is a decrease in HC emissions upto 25 to 30% of biodiesel blends; beyond that, increased FB leads to increased HC emissions. Maximum HC was seen at 60% FB, which is considerably reduced by the increase of supplied fuel injection pressure. The high injection pressure turns into a fine spray and reduces the viscosity; therefore, mixing with air is very easy, so better combustion is possible than low injection pressure.

HC (PPM vol)

Design Points:

- Above Surface
- Below Surface

7  23

X1 = B

X2 = D

Actual Factors

A = 30

C = 700

E = 8

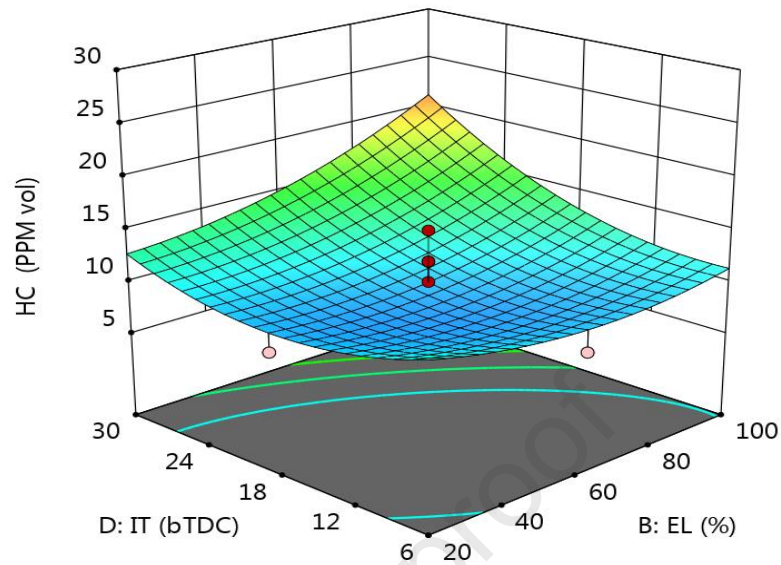



Figure 19: effect of IT, EL on HC

For the various engine load and injection timing corresponding, HC emissions is shown in figure 19. The maximum hydrocarbon emission was seen when conducting an experiment at a higher engine load and injecting fuel too away from TDC. At a full load of engine operation by advancing fuel injection from 6 to 30 degree before TDC there is a considerable increase in HC emission. At 30 degree before TDC increasing EL from 20 to 100% of engine load, there is a substantial increase in HC emission. The high density and viscosity of grape seed biodiesel blended fuel will not mix properly with compressed air, leading to poor combustion.

HC (PPM vol)
 Design Points:
 ● Above Surface
 ○ Below Surface
 7  23

X1 = B
 X2 = E

Actual Factors
 A = 30
 C = 700
 D = 18

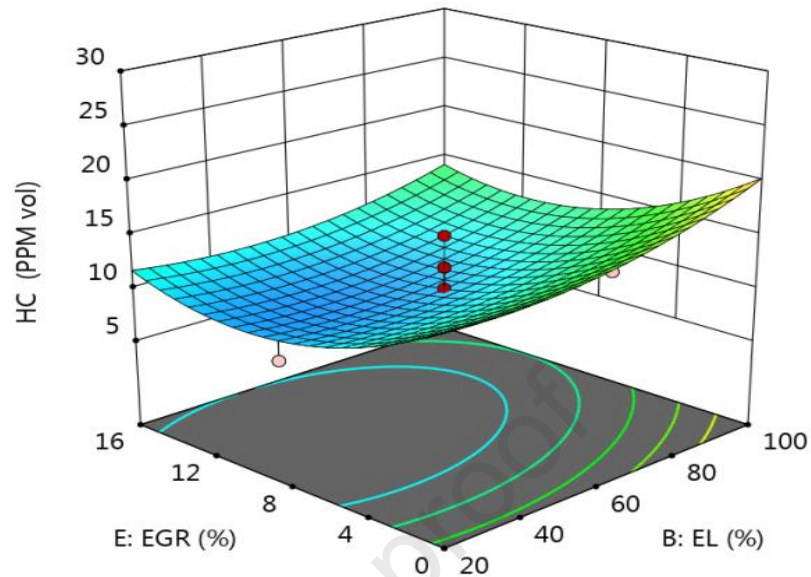


Figure 20: effect of EGR, EL on HC

EGR versus EL effect on hydrocarbon emission is shown in figure 20. Even with EGR upto 16%, the reported HC emission was lower than without re-circulating exhaust gas inside the combustion cylinder at the entire load operation of the engine. Small Addition of EGR turns initially decreases in HC emission. Still, after a specific limit, there is slight stagnancy in HC emission, so there is space for the researcher to find the optimum combination. The inlet air temperature slightly increases due to the addition of EGR, resulting in better combustion and lower HC formation at full load than without the addition of EGR.

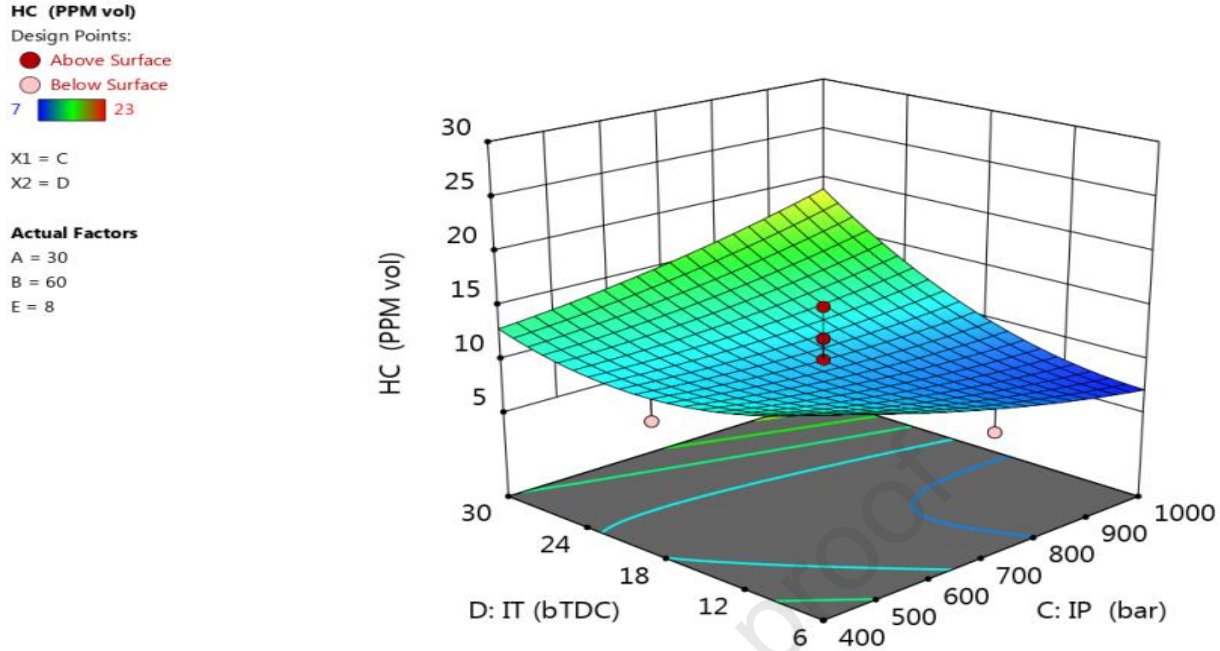


Figure 21: effect of IT, IP on HC

IT versus IP effect on HC response is shown in figure 21. The lowest and highest HC was seen at 1000bar IP, 6 degree before TDC and 1000bar, 30 degree before TDC. At 1000bar IP, injecting the fuel at various injections timing 6 to 30 degree before TDC turns into a gradual increase of HC emission. Similarly, at 30 degree before TDC with the rise of IP 400 to 1000bar, there was a considerable increase in HC emissions due to unfavorable combustion situations for the considered parameter constraints.

$$\begin{aligned}
 \text{HC} = & 38.0001 + -0.284444 * \text{FB} + -0.210729 * \text{EL} + -0.0224444 * \text{C} + -1.35937 * \text{IT} + 0.0229167 \\
 & * \text{EGR} + 0.0015625 * (\text{FB} * \text{EL}) + -0.000180556 * (\text{FB} * \text{IP}) + 0.00590278 * (\text{FB} * \text{IT}) + -0.0140625 \\
 & * (\text{FB} * \text{EGR}) + 1.04167\text{e-}05 * (\text{EL} * \text{IP}) + 0.00494792 * (\text{EL} * \text{IT}) + -0.00195313 * (\text{EL} * \text{EGR}) + \\
 & 0.0009375 * (\text{IP} * \text{IT}) + -0.000260417 * (\text{IP} * \text{EGR}) + -0.0299479 * (\text{IT} * \text{EGR}) + 0.00636111 * \text{A}^2 \\
 & + 0.00107812 * \text{EL}^2 + 8.05556\text{e-}06 * \text{IP}^2 + 0.0189236 * \text{IT}^2 + 0.0582031 * \text{EGR}^2
 \end{aligned}$$

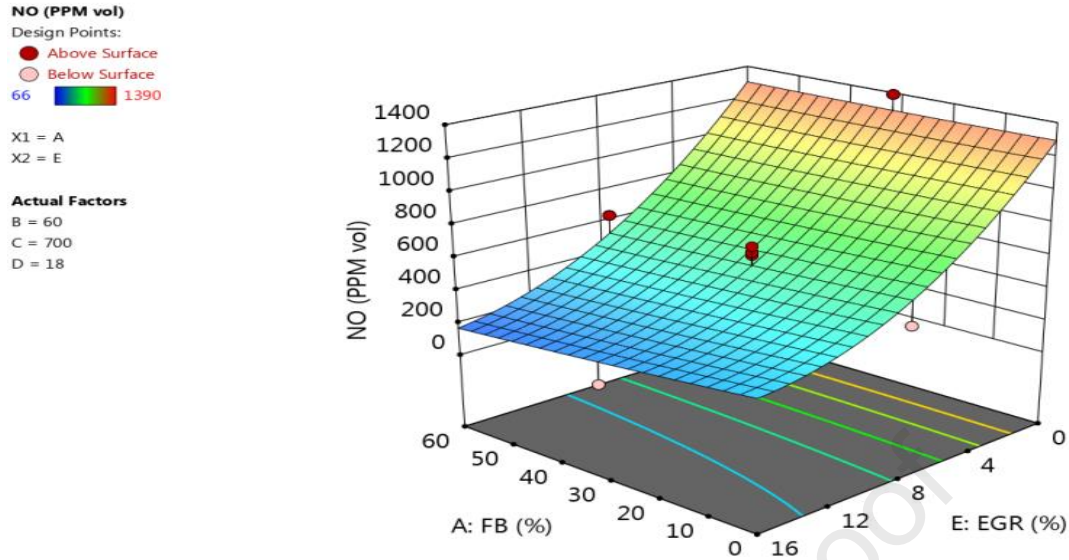


Figure 22: effect of FB, EGR on NO_x

With the incremental addition of EGR rate by 4% from 0 to 16%, a tremendous decrease in NO_x pollutants was seen, as shown in figure 22. The lowest NO_x was seen at the operating condition of 60% FB and 16% of EGR rate due to inadequate combustion temperature. NO_x formation occurs mainly at high temperatures. Therefore, introducing EGR in the combustion chamber creates a shortage of oxygen, leading to a poor combustion reaction. In addition, EGR with biodiesel blends causes low combustion temperature at a high level of EGR. Still, there is no significant change without adding EGR. 66 and 1390ppm were the highest and lowest NO_x seen during experimentation.

$$\begin{aligned} \text{NO}_x = & -467.456 + -0.103889 * \text{FB} + 11.7157 * \text{EL} + 1.29022 * \text{IP} + 47.0233 * \text{IT} + -38.9125 * \\ & \text{EGR} + 0.0430208 * (\text{FB} * \text{EL}) + -0.000486111 * (\text{FB} * \text{IP}) + -0.137847 * (\text{FB} * \text{IT}) + -0.164063 * \\ & (\text{FB} * \text{EGR}) + 0.00536458 * (\text{EL} * \text{IP}) + 0.15026 * (\text{EL} * \text{IT}) + -0.784766 * (\text{EL} * \text{EGR}) + -0.0281597 \\ & * \text{IP} * \text{IT}) + 0.0145312 * \text{IP} * \text{EGR}) + -2.14453 * (\text{IT} * \text{EGR}) + 0.00697222 * \text{FB}^2 + -0.125453 * \\ & \text{EL}^2 + -0.000730278 * \text{IP}^2 + 0.269271 * \text{IT}^2 + 3.34805 * \text{EGR}^2 \end{aligned}$$

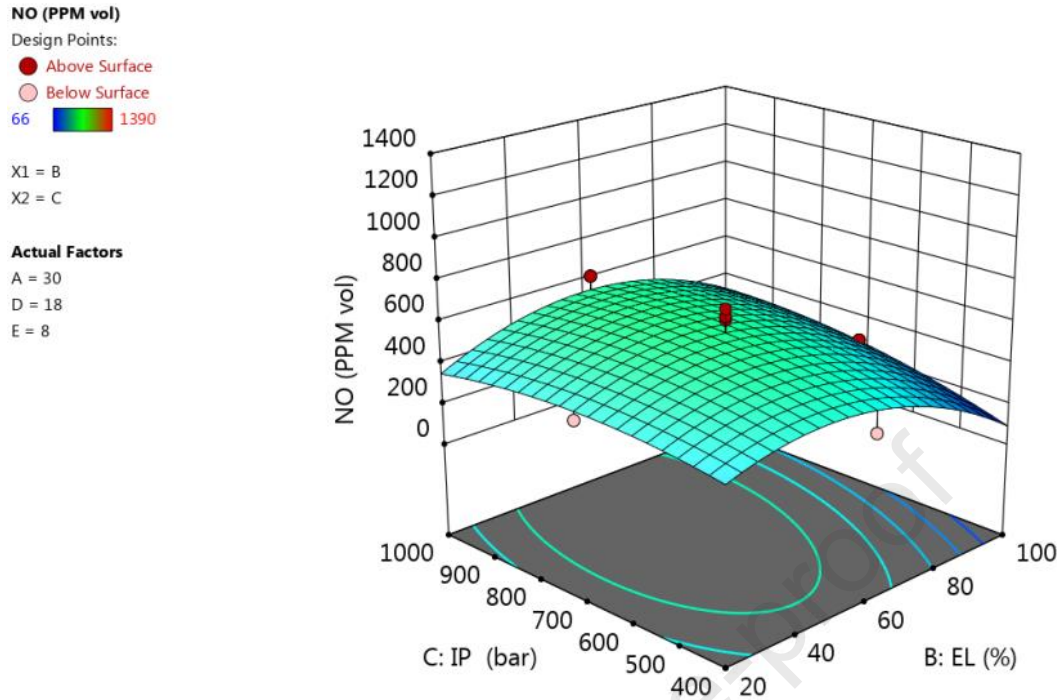


Figure 23: effect of IP, EL on NO_x

The engine output response of NO_x when varying the engine load versus injection pressure is shown in figure 23. Based on the design of the experiment-based run, it is observed that change of injection pressure towards 1000 bar from 400 bar with an increment of 150 bar there is no more significant effect on NO_x formation for all the loads of operations. Still, the maximum NO_x was observed at 60% of engine load and around 800 bar injection pressure. Also, when increasing engine load, NO_x emissions increase upto 60% EL; beyond that, NO_x emissions start to decrease for all the injection pressure ranges. Until the certain injection pressure level, there is an efficient combustion reaction, and beyond that level, no much more significant NO_x emission was reported. Therefore, optimum injection pressure for the chosen parameters needs to be evaluated.

NO (PPM vol)

Design Points:

● Above Surface

○ Below Surface

66  1390

X1 = A

X2 = D

Actual Factors

B = 60

C = 700

E = 8

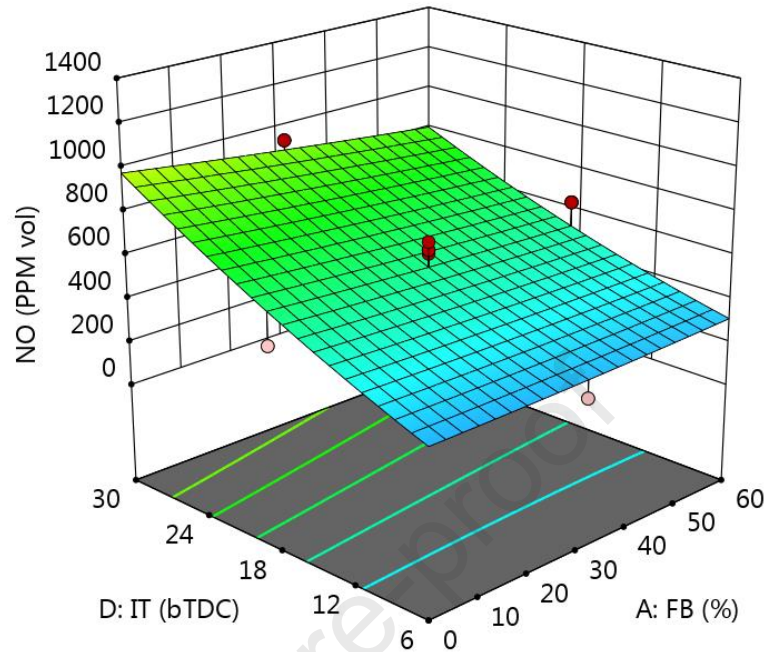


Figure 24: effect of IT, FB on NO_x

Advancing fuel IT from 6 to 30 degree before the top dead center, the reported responses of NO_x tremendously raised, then this rise in emission was considerably reduced with the increase in addition of biodiesel blend such as 0%, 15%, 30%, 45%, and 60%, due to lower calorific value than baseline diesel fuel. For all the experimental fuel samples, Injection of fuel just nearer to TDC produces lower NO_x than injecting too away from TDC due to quiet residence time causes moderate combustion effect turns into lower combustion temperature as shown in figure 24. An advanced injection leading to proper mixing result in attains the NO_x formation reaction temperature limits. At 6 degree bTDC for all the test fuel samples, there is not much effect as seen at 30 degree bTDC. Therefore, injecting fuel near TDC gives favorable NO_x emissions rather than advancing the fuel injection timing away from TDC.

SFC (kg/kWh)

Design Points:

● Above Surface

○ Below Surface

0.24 0.66

X1 = B

X2 = C

Actual Factors

A = 30

D = 18

E = 8

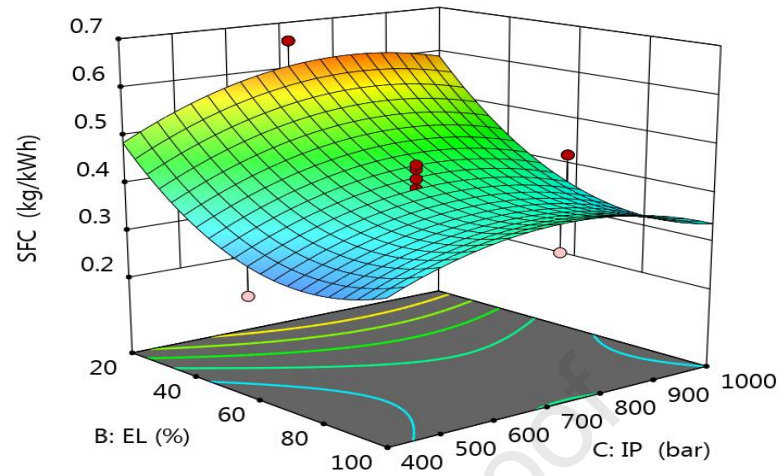


Figure 25: effect of EL, IP on SFC

The interactive effect of EL versus IP on SFC is shown in figure 25. Increasing engine load corresponding energy demand is fulfilled by extraction of energy, by proper combustion of fuel. Hence fuel requirement at a higher load is lesser than a low operation load for all the fuel injection pressure. From the graph, it is clear that with increasing IP, there is a corresponding increase in SFC, but fuel consumption started to decrease considerably beyond a certain level. So there is some opportunity for the researcher to identify the optimum combination.

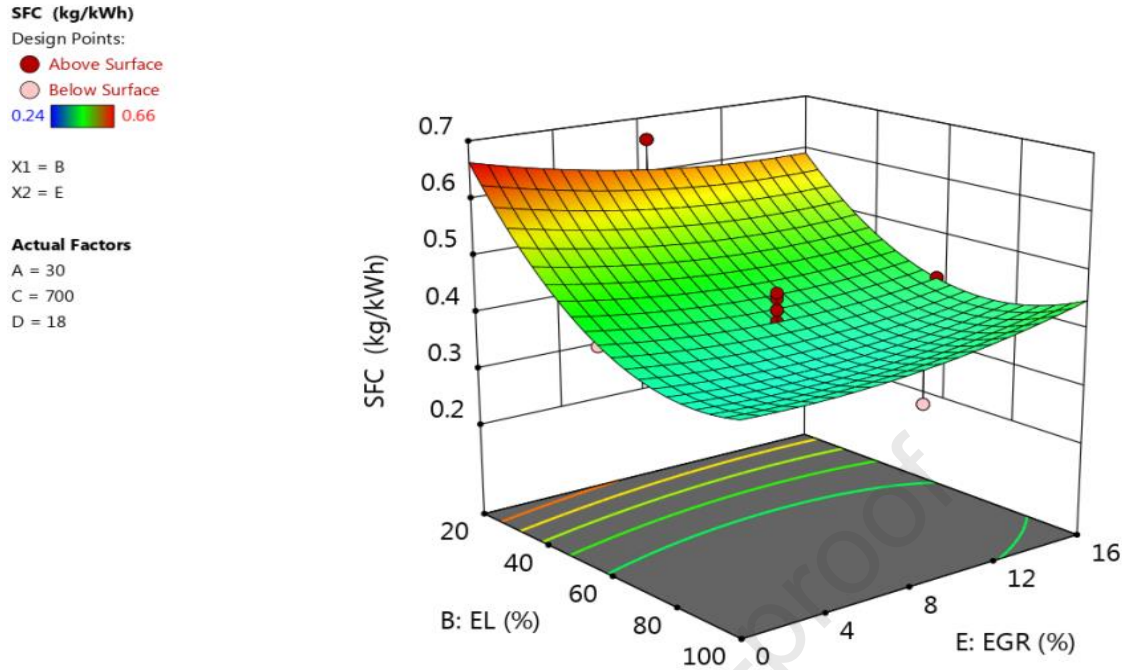


Figure 26: effect of EL, EGR on SFC

In the normal thermodynamic cyclic process of engine operation, when the exhaust gas is recirculated with the increment of 4% from 0% to 16%, there was a considerable increase in SFC requirement at full load. A decrease in SFC was seen with the addition of EGR at a low operation load, as shown in figure 26. Therefore optimum EGR percentage rate needs to be investigated throughout the engine load ranges by considering all other influencing parameters. To fulfill the required thrust at full load slight increase in fuel consumption was reported to overcome EGR introduced the effect of lower combustion rate due to shortage of oxygen leads to improper combustion.

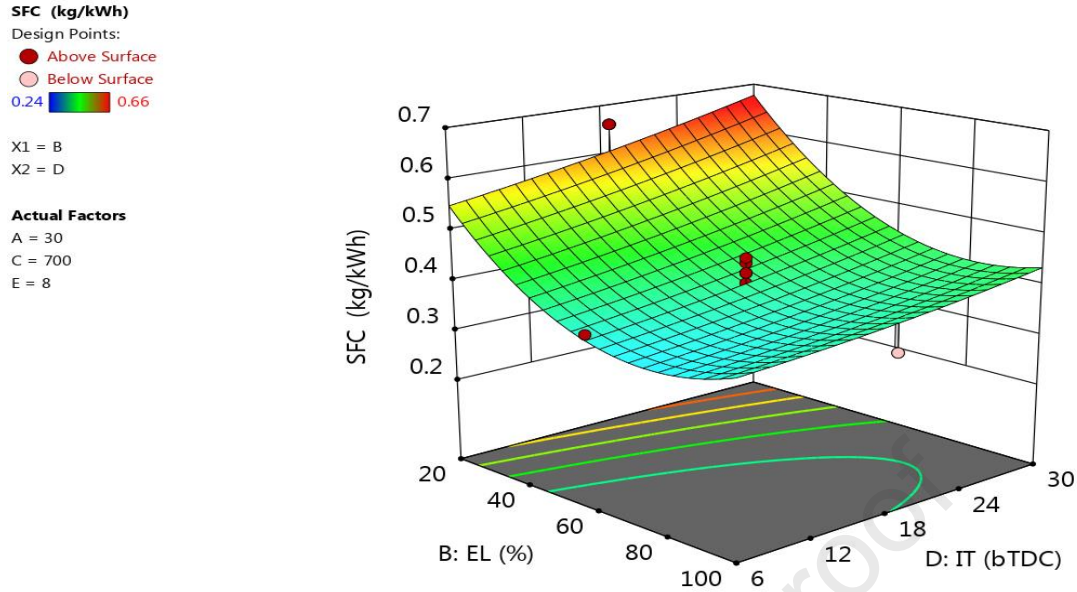


Figure 27: effect of EL, IT on SFC

The interactive effect of EL versus IT on SFC is shown in figure 27. For all the loads of engine operation with the advancement of fuel injection by the interval of 6 degree from 6 to 30 degree before the top dead center resulted in a significant increment in requirement of SFC. In low load of operation, all the fuel energy is not utilized as in a high load of the cyclic process; therefore, higher SFC occurs at a low load. The lower SFC was reported when operating the engine towards the maximum load and injecting fuel near TDC before advancing FIT. Early injection causes certain rise in pressure before the piston reaching TDC leading to more energy consumption but actually pressure rise required at the TDC.

SFC (kg/kWh)

Design Points:

● Above Surface
○ Below Surface
0.24 0.66

X1 = A

X2 = B

Actual Factors

C = 700

D = 18

E = 8

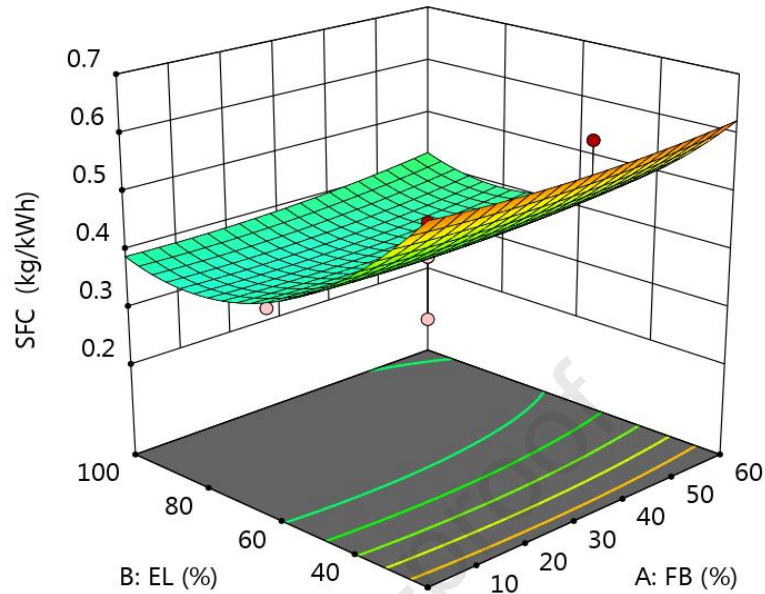


Figure 28: effect of EL, FB on SFC

With the increase in engine load, there was a considerably tremendous decrease in SFC of the engine, as shown in figure 28. It was seen that the biodiesel blend percentage increase causes a slight rise of SFC towards at full load of operation due to the lower calorific nature, high density and viscosity of the prepared grape seed biodiesel blend. There is no considerable increase of SFC for biodiesel blend for all loads of process than diesel alone as fuel. At full load, even the addition of 60% biofuel in diesel reported lower brake SFC than the low load of operation without biofuel blend.

$$\begin{aligned} \text{SFC} = & 0.303751 + -0.00104444 * \text{FB} + -0.00943229 * \text{EL} + 0.00126389 * \text{IP} + 0.000878472 * \text{IT} \\ & + -0.0136667 * \text{EGR} + 5.20833\text{e-}06 * (\text{FB} * \text{EL}) + -1.80556\text{e-}06 * (\text{FB} * \text{IP}) + 7.98611\text{e-}05 * \\ & (\text{FB} * \text{IT}) + 1.5625\text{e-}05 * (\text{FB} * \text{EGR}) + -1.77083\text{e-}06 * (\text{EL} * \text{IP}) + -3.38542\text{e-}05 * (\text{EL} * \text{IT}) + \\ & 0.000105469 * (\text{EL} * \text{EGR}) + 1.73611\text{e-}06 * (\text{IP} * \text{IT}) + 2.60417\text{e-}06 * (\text{IP} * \text{EGR}) + -3.90625\text{e-}05 * \\ & (\text{IT} * \text{EGR}) + 1.36111\text{e-}05 * \text{FB}^2 + 6.39062\text{e-}05 * \text{EL}^2 + -7.52778\text{e-}07 * \text{IP}^2 + 5.03472\text{e-}05 * \\ & \text{IT}^2 + 0.000347656 * \text{EGR}^2 \end{aligned}$$

RSM and ANN Analysis

The parameter considered for this analysis for improving the performance of the engine, such as FB, EL, IP, IT, and EGR as influencing parameters of the CRDI engine and the output process responses such as SFC, BMEP, BTHE, Mech. Effi., CO, HC, NOx. Numerical optimization was done in the way of improving performance characteristics and to reduce the emission nature of CRDI engine run with blends of grape seed biodiesel and the details about the importance of different responses considered for evaluation as well as the desirability of each parameter to fulfill the goal is shown in table 9. Multi-objective numerical optimization in engine performance with different sources of biodiesel has been done by (Ramalingam et al. 2022), (Teoh et al. 2021), and the second order equations can be done by RSM (Sharma, Singh, Kumar Singh, et al. 2020), (Sharma, Singh, Tyagi, et al. 2020). Different methods are used in developing the design matrix in RSM, and an effective way is the central composite design (S. Kumar and Dinesha 2018). CRDI engine parameters were analyzed by RSM based tool using linseed biodiesel (M. Kumar et al. 2022). RSM Optimized result is shown in figure 29. The maximum combined desirability of 0.824 was seen when adjusting the input engine setting of 33.3% of grape seed biodiesel blend, 82% of engine load, 1000 bar of injection pressure, and 6-degree bTDC of injection timing, 6.7% of EGR. The individual desirability of each response is shown in table 9. Confirmatory experimental run conducted at the optimum combination and the error percentage between experimental and predicted for all the output is less than 5% as shown in table 11.

Table 9: Goal, weightage, and desirability of RSM analysis

| Name | Goal | Lower Limit | Upper Limit | Lower Weight | Upper Weight | Importance | Desirability |
|-------------|-------------|-------------|-------------|--------------|--------------|------------|--------------|
| A:FB | is in range | 0 | 60 | 1 | 1 | 3 | 1 |
| B:EL | is in range | 20 | 100 | 1 | 1 | 3 | 1 |
| C:IP | is in range | 400 | 1000 | 1 | 1 | 3 | 1 |
| D:IT | is in range | 6 | 30 | 1 | 1 | 3 | 1 |
| E:EGR | is in range | 0 | 16 | 1 | 1 | 3 | 1 |
| SFC | minimize | 0.24 | 0.66 | 1 | 1 | 3 | 0.91 |
| BMEP | maximize | 0.89 | 4.24 | 1 | 1 | 3 | 0.8 |
| BTHE | maximize | 13.3 | 34.74 | 1 | 1 | 3 | 0.93 |
| Mech. Effi. | maximize | 25.98 | 68.87 | 1 | 1 | 3 | 0.89 |

| | | | | | | | |
|-----|----------|------|------|---|---|---|------|
| CO | minimize | 0.04 | 0.32 | 1 | 1 | 3 | 0.57 |
| HC | minimize | 7 | 23 | 1 | 1 | 3 | 0.96 |
| NOx | minimize | 66 | 1390 | 1 | 1 | 3 | 0.78 |

Table 10: Comparisons of R-value of ANN and RSM

| | SFC | BMEP | BTHE | MECH. Effi. | CO | HC | NO |
|---------------------------------------|------|------|------|----------------|-------------|------|-------|
| R (ANN) | 0.88 | 0.99 | 0.84 | 0.99 | 0.9657 1 | 0.76 | 0.948 |
| Hidden layer | 6 | 2 | 13 | 4 | 19 | 3 | 3 |
| Epoch Iterations | 9 | 67 | 7 | 28 | 6 | 10 | 10 |
| R (RSM) | 0.79 | 0.99 | 0.77 | 0.98 | 0.94 | 0.71 | 0.91 |
| ANN % prediction accuracy than RSM | 11.4 | 0 | 9.1 | 1.02 | 2.73 | 7.04 | 4.175 |

Table 11: error of experimental and predicted value

| | FB (%) | EL (%) | IP (bar) | IT (bTDC) | EGR (%) | BMEP (bar) | BTE (%) | Mech Eff. (%) | SFC (kg/kWh) | CO in % | NOx (PPM) | HC (PPM) |
|-----------|-----------|---------|-------------|--------------|------------|---------------|------------|------------------|-----------------|------------|--------------|-------------|
| Exp. | 33 | 82 | 1000 | 6 | 7 | 3.49 | 30.44 | 63.23 | 0.289 | 0.132 | 366 | 8 |
| Predicted | 33.3 | 82.0015 | 999.98 | 6 | 6.707 | 3.559 | 31.85 | 64.0609 | 0.278 | 0.1277 | 356.8 | 7.64 |
| Error (%) | | | | | | 2.05 | 4.600 | 1.31 | 3.917 | 3.03 | 2.496 | 4.5 |

Table 12: Design of experiment

| Random Run | FB (%) | EL(kg) | FIP(MPa) | FIT(°bTDC) | EGR (%) |
|---------------|--------|--------|----------|------------|---------|
| 1 | 30 | 7.4 | 70 | 18 | 8 |
| 2 | 45 | 9.8 | 55 | 24 | 12 |
| 3 | 45 | 4.9 | 85 | 12 | 4 |
| 4 | 45 | 4.9 | 55 | 24 | 4 |
| 5 | 45 | 4.9 | 55 | 24 | 12 |

| | | | | | |
|----|----|------|-----|----|----|
| 6 | 45 | 4.9 | 85 | 24 | 12 |
| 7 | 15 | 9.8 | 55 | 12 | 12 |
| 8 | 45 | 9.8 | 85 | 12 | 12 |
| 9 | 45 | 9.8 | 85 | 12 | 4 |
| 10 | 15 | 4.9 | 85 | 24 | 12 |
| 11 | 30 | 7.4 | 70 | 18 | 8 |
| 12 | 45 | 4.9 | 85 | 24 | 4 |
| 13 | 45 | 4.9 | 85 | 12 | 12 |
| 14 | 15 | 4.9 | 55 | 12 | 4 |
| 15 | 45 | 4.9 | 55 | 12 | 12 |
| 16 | 45 | 9.8 | 55 | 24 | 4 |
| 17 | 30 | 2.5 | 70 | 18 | 8 |
| 18 | 30 | 7.4 | 70 | 18 | 16 |
| 19 | 30 | 7.4 | 70 | 18 | 8 |
| 20 | 15 | 9.8 | 85 | 24 | 12 |
| 21 | 15 | 9.8 | 85 | 12 | 4 |
| 22 | 45 | 9.8 | 55 | 12 | 12 |
| 23 | 45 | 4.9 | 55 | 12 | 4 |
| 24 | 30 | 7.4 | 70 | 18 | 8 |
| 25 | 30 | 7.4 | 100 | 18 | 8 |
| 26 | 30 | 7.4 | 70 | 18 | 8 |
| 27 | 30 | 7.4 | 70 | 30 | 8 |
| 28 | 30 | 12.3 | 70 | 18 | 8 |
| 29 | 15 | 4.9 | 85 | 12 | 4 |
| 30 | 30 | 7.4 | 70 | 6 | 8 |
| 31 | 15 | 9.8 | 55 | 24 | 4 |
| 32 | 15 | 9.8 | 55 | 24 | 12 |

| | | | | | |
|----|----|-----|----|----|----|
| 33 | 45 | 9.8 | 85 | 24 | 12 |
| 34 | 15 | 4.9 | 55 | 12 | 12 |
| 35 | 0 | 7.4 | 70 | 18 | 8 |
| 36 | 15 | 4.9 | 85 | 12 | 12 |
| 37 | 15 | 4.9 | 55 | 24 | 12 |
| 38 | 15 | 9.8 | 55 | 12 | 4 |
| 39 | 30 | 7.4 | 40 | 18 | 8 |
| 40 | 15 | 4.9 | 85 | 24 | 4 |
| 41 | 30 | 7.4 | 70 | 18 | 8 |
| 42 | 45 | 9.8 | 55 | 12 | 4 |
| 43 | 30 | 7.4 | 70 | 18 | 8 |
| 44 | 15 | 9.8 | 85 | 12 | 12 |
| 45 | 45 | 9.8 | 85 | 24 | 4 |
| 46 | 30 | 7.4 | 70 | 18 | 8 |
| 47 | 60 | 7.4 | 70 | 18 | 8 |
| 48 | 15 | 4.9 | 55 | 24 | 4 |
| 49 | 15 | 9.8 | 85 | 24 | 4 |
| 50 | 30 | 7.4 | 70 | 18 | 0 |

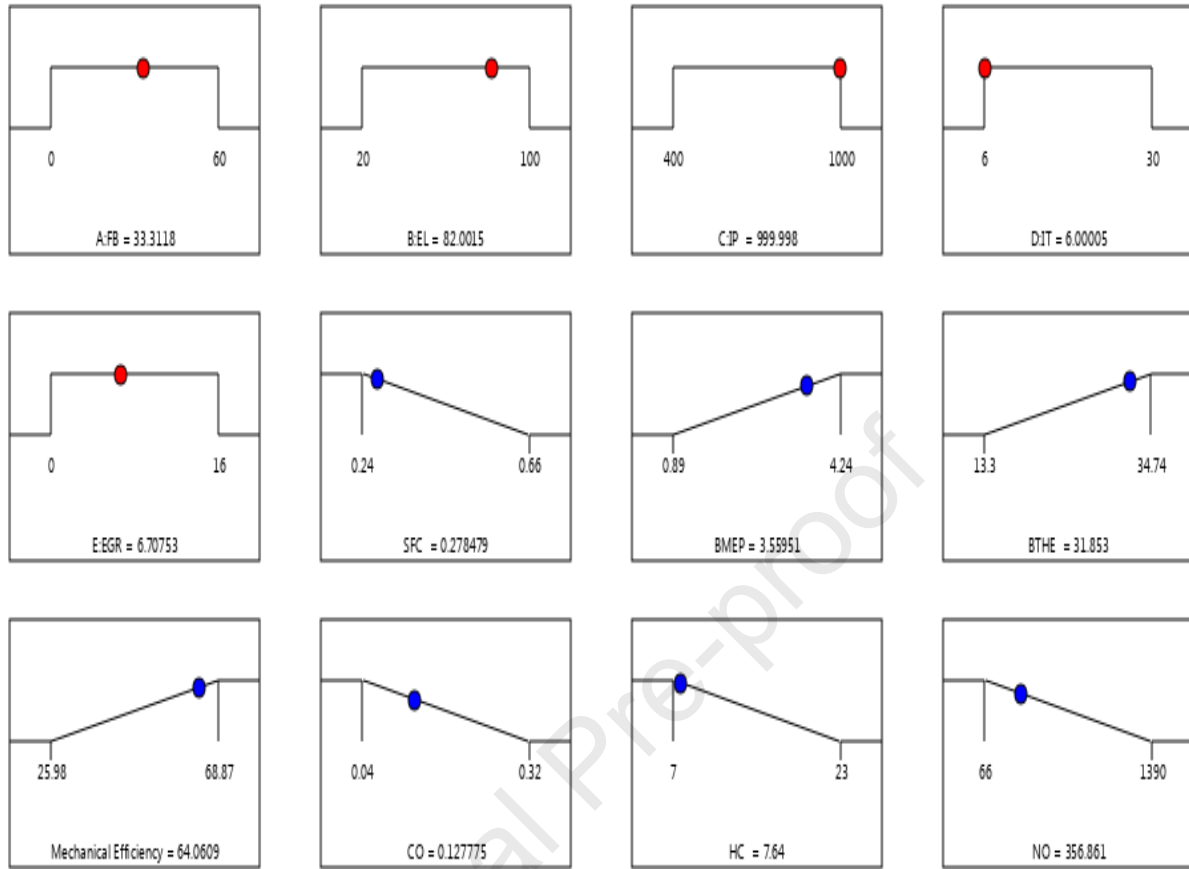


Figure 29: RSM optimized result

An artificial Neural Network algorithm was used to predict engine output responses. Random dividerand data division, levenberg-marquardt training, mean squared error performance, and MEX calculations were used in the algorithm. Training, validation, and test regression analysis were performed by changing the hidden layer until the desired predicted regression values were obtained. The predicted value of each engine output response is more accurate in ANN than response surface methodology-based prediction. Neural network-based prediction are 11.4%, 9.1%, 1.02%, 2.73%, 7.04%, 4.175% higher than RSM prediction for SFC, BTHE, MECH. Efficiency, CO, HC, and NO_x, respectively, and the comparison of ANN versus RSM is shown in table 10.

CONCLUSIONS

Experimental work is done in CRDI engine supplying grape seed biodiesel at fixed compression ratio 18, speed 1500 rpm by varying main influencing parameters, and after 50 input combination variation run in engine, the following conclusions are drawn.

- Biodiesel was made in accordance with ASTM standards, and the test fuel characteristics of the prepared biodiesel were discovered to be within ASTM standard criteria.
- Design expert software was used for the development of the RSM (central composite type design) experimental matrix of 50 input combinations.
- RSM was utilised for forecasting and to develop a second-order quadratic equations for each engine outputs responses, such as BMEP, mech. effi., BTE, BSFC, CO, HC, and NO_x.
- EL is the primary influencing parameter for torque, BP, BMEP, and mechanical efficiency. The remaining parameters have the least influence on these parameters. Apart from types of fuel used, at high IP, the Torque, BP, BMEP are depends primarily on EL.
- At high injection pressure fueled operations, the EL and FIT possess more influence on controlling engine efficiency than other parameters considered.
- Air pressure and temperature are higher near TDC than they are at the beginning of the compression process, which results in better air-fuel mixing near TDC than they were earlier in the process. Better combustion, in turn, causes an increase in BTE and a decrease in SFC at high loads.
- When operating at high injection pressures (40–100 MPa), enhanced BTE results from above-half loads near TDC injection and below-half loads in the early stages of fuel injection during the compression process.
- Low load energy requirements are met by biodiesel blends alone in high IP operations (40–100 MPa), but above half load, somewhat lower BTE and higher SFC are noted due to lower energy density than in diesel fuel operations.
- An ANOVA study helps identify the parameters that have the maximum influence on each output response. EL has 1.21, 6.10, 64.40, 69, 94, 68, and 99.9 percentage influences on

NO_x, HC, CO, SFC, Mech. effi., BTE, and BMEP. FB has a 5.4% influence on HC. IT has 26%, 12.61%, 12.56%, 2%, 11.58%, and 19% influence on friction power, BTE, SFC, CO, HC, and NO_x. EGR has 89%, 7%, 11%, and 60% influence on vol. effi., CO, HC, and NO_x.

- A learning-based ANN technique was used to predict outcomes, and the projected values were more accurate than RSM. ANN could be more successfully used for predicting output responses than the prediction by RSM via. Neural network-based prediction are 11.4%, 9.1%, 1.02%, 2.73%, 7.04%, 4.175% higher than RSM prediction for SFC, BTHE, mech. efficiency, CO, HC, and NO_x, respectively
- Using the RSM desirability approach, the optimal settings for the CRDI engine were determined to yield improved reactions. These settings included 1000 bar of IP, 6°bTDC of IT, 33% of a mix of grape biodiesel with 77% diesel, 6.7% of EGR, and 82% engine load. These ideal input conditions resulted in engine outputs of 3.55 bar BMEP, 31.85% BTE, 64% mechanical efficiency, 0.278 kg/kWh SFC, 0.127% CO, 357 ppm NO_x, and 8 ppm HC.
- The RSM desirability method-based optimal engine operation employing diesel mixed with GSB is validated using experiments at the optimal settings, and the error between experiment and RSM is less than 5%.
- When operating engine at 60% EL, 70 MPa IP, 18° bTDC, 8% EGR, The addition of grape seed biodiesel to diesel increases the oxygen presence in the prepared fuel, allowing for a complete combustion reaction. However, excessive addition of low-calorific grape seed biodiesel to diesel results in lower energy density, which leads to GSB B60 reporting lower peak cylinder pressure than GSB B30 and diesel. The GSB B30 has a 0.5% greater peak cylinder pressure than the diesel. However, the GSB B60 has a 1.1% lower peak cylinder pressure than the diesel.
- The investigation's optimal outcome is only suitable for the 1500 rpm, and CR 18:1 of the CRDI engine, with various input parameter ranges and output parameters considered.
- The use of second-generation Grape biofuel is a substitute for potential applications for

better economic and environmental aspects hence this can be used as an emergency or alternative fuel for diesel engines. Hence recommending engine manufacturers to design or end users to operate at this optimum conditions.

Future work

Blending of second-generation biofuel with third and fourth generation biofuel in the aspect of enhancing the quality of biofuel and evaluate the efficiency characteristics and identifying optimum conditions by considering all the possible real time affecting parameters as future scope of this work.

References

- Azad, Kalam, and Mohammad Rasul. 2019. "Performance and Combustion Analysis of Diesel Engine Fueled with Grape Seed and Waste Cooking Biodiesel." *Energy Procedia* 160 (2018): 340–47. <https://doi.org/10.1016/j.egypro.2019.02.166>.
- Dond, Dipak Kisan, and Nitin Parashram Gulhane. 2021. "Optimization of Injection System Parameter for CRDI Small Cylinder Diesel Engine by Using Response Surface Method." *Journal of The Institution of Engineers (India): Series C* 102 (4): 1007–29. <https://doi.org/10.1007/s40032-021-00688-6>.
- DUDA, Kamil, Sławomir WIERZBICKI, Maciej MIKULSKI, Łukasz KONIECZNY, Bogusław ŁAZARZ, and Magdalena LETUŃ-ŁĄTKA. 2021. "Emissions from a Medium-Duty Crdi Engine Fuelled with Diesel-Biodiesel Blends." *Transport Problems* 16 (1): 39–49. <https://doi.org/10.21307/tp-2021-004>.
- Fadairo, Adebayo, and Weng Fai Ip. 2021. "A Study on Performance Evaluation of Biodiesel from Grape Seed Oil and Its Blends for Diesel Vehicles." *Vehicles* 3 (4): 790–806. <https://doi.org/10.3390/vehicles3040047>.
- Ganji, Prabhakara Rao, Kiran Prasad Chintala, V. R.K. Raju, and Srinivasa Rao Surapaneni. 2017. "Parametric Study and Optimization Using RSM of DI Diesel Engine for Lower Emissions." *Journal of the Brazilian Society of Mechanical Sciences and Engineering* 39 (3): 671–80.

<https://doi.org/10.1007/s40430-016-0600-0>.

- Hariram, V., A. Bose, and S. Seralathan. 2019. "Dataset on Optimized Biodiesel Production from Seeds of *Vitis Vinifera* Using ANN, RSM and ANFIS." *Data in Brief* 25: 104298. <https://doi.org/10.1016/j.dib.2019.104298>.
- Kanthasamy, P., V. Arul Mozhi Selvan, and P. Shanmugam. 2020. "Investigation on the Performance, Emissions and Combustion Characteristics of CRDI Engine Fueled with Tallow Methyl Ester Biodiesel Blends with Exhaust Gas Recirculation." *Journal of Thermal Analysis and Calorimetry* 141 (6): 2325–33. <https://doi.org/10.1007/s10973-020-09770-0>.
- Karthikeyan, S., A. Prathima, A. Elango, and S. M. Silaimani. 2015. "Environmental Effect of *Vitis Vinifera* (Grape Seed Oil) Biofuel Blends in Marine Engine." *Indian Journal of Geo-Marine Sciences* 44 (12): 1852–56.
- Kulandaivel, D., I. G. Rahamathullah, A. P. Sathiyagnanam, K. Gopal, D. Damodharan, and De Poures Melvin Victor. 2020. "Effect of Retarded Injection Timing and EGR on Performance, Combustion and Emission Characteristics of a CRDi Diesel Engine Fueled with WHDPE Oil/Diesel Blends." *Fuel* 278 (June): 118304. <https://doi.org/10.1016/j.fuel.2020.118304>.
- Kumar, Manish, Varun Kumar Singh, Abhishek Sharma, Naushad Ahmad Ansari, Raghvendra Gautam, and Yashvir Singh. 2022. "Effect of Fuel Injection Pressure and EGR Techniques on Various Engine Performance and Emission Characteristics on a CRDI Diesel Engine When Run with Linseed Oil Methyl Ester." *Energy and Environment* 33 (1): 41–63. <https://doi.org/10.1177/0958305X20983477>.
- Kumar, Prashanth, Nagaraj R. Banapurmath, Peter Fernandes, and Raju K. 2019. "Influence of Injection Strategy on B20MOME Fueled CRDI Engine with Toroid Shaped Piston Cavity." *European Journal of Sustainable Development Research* 3 (3). <https://doi.org/10.20897/ejosdr/3974>.
- Kumar, Shiva, and P. Dinesha. 2018. "Optimization of Engine Parameters in a Bio Diesel Engine Run with Honge Methyl Ester Using Response Surface Methodology." *Measurement: Journal of the International Measurement Confederation* 125 (September): 224–31. <https://doi.org/10.1016/j.measurement.2018.04.091>.

- N., Keerthi Kumar, N. R. Banapurmath, T. K. Chandrashekar, Jatadhara G. S., Manzoore Elahi M. Soudagar, Ali E. Anqi, M. A. Mujtaba, et al. 2021. "Effect of Parameters Behavior of Simarouba Methyl Ester Operated Diesel Engine." *Energies* 14 (16): 4973. <https://doi.org/10.3390/en14164973>.
- Ong, Hwai Chyuan, M. Mofijur, A. S. Silitonga, D. Gumilang, Fitrinto Kusumo, and T. M.I. Mahlia. 2020. "Physicochemical Properties of Biodiesel Synthesised from Grape Seed, Philippine Tung, Kesambi, and Palm Oils." *Energies* 16 (3). <https://doi.org/10.3390/en13061319>.
- Raeie, Nader, Sajjad Emami, and Omid Karimi Sadaghiyani. 2014. "Effects of Injection Timing, before and after Top Dead Center on the Propulsion and Power in a Diesel Engine." *Propulsion and Power Research* 3 (2): 59–67. <https://doi.org/10.1016/j.jprr.2014.06.001>.
- Ramachander, J., S. K. Gugulothu, G. R.K. Sastry, Jibitesh Kumar Panda, and M. Siva Surya. 2021. "Performance and Emission Predictions of a CRDI Engine Powered with Diesel Fuel: A Combined Study of Injection Parameters Variation and Box-Behnken Response Surface Methodology Based Optimization." *Fuel* 290 (April). <https://doi.org/10.1016/j.fuel.2020.120069>.
- Ramalingam, Sathiyamoorthi, Sankaranarayanan Gomathinayakam, Venkatraman Mani, Jayaseelan Veerasundaram, and Sivakumar Kachapalayam. 2022. "Analysis of Optimising Injection Parameters and EGR for DICI Engine Performance Powered by Lemongrass Oil Using Box–Behnken (RSM) Modelling." *International Journal of Ambient Energy*, January, 1–18. <https://doi.org/10.1080/01430750.2021.2019111>.
- Sankar Ganesh, R., B. Ganesh Babu, and Ragupathy Karu. 2019. "Experimental Investigations on Direct Injection Diesel Engines Using Grape Seed Oil Methyl Ester with Different Bowl Geometries." *International Journal of Green Energy* 16 (8): 590–97. <https://doi.org/10.1080/15435075.2019.1601095>.
- Sathiyamoorthi, R, A Anbarasu, M Dinesh Babu, and V Rajangam. 2019. "Optimization of Injection Parameters and Compression Ratio on a Single Cylinder Diesel Engine Fuelled by Azadirachta Indica (Neem) Biodiesel Using Response Surface Methodology (RSM)."

Journal of Applied Science and Computations 6 (4): 21–28.

Serio, Domenico De, Alex de Oliveira, and José Ricardo Sodr . 2017. “Effects of EGR Rate on Performance and Emissions of a Diesel Power Generator Fueled by B7.” *Journal of the Brazilian Society of Mechanical Sciences and Engineering* 39 (6): 1919–27. <https://doi.org/10.1007/s40430-017-0777-x>.

Shanmugam, Rajasekaran, Damodharan Dillikannan, Gopal Kaliyaperumal, Melvin Victor De Poures, and Rajesh Kumar Babu. 2021. “A Comprehensive Study on the Effects of 1-Decanol, Compression Ratio and Exhaust Gas Recirculation on Diesel Engine Characteristics Powered with Low Density Polyethylene Oil.” *Energy Sources, Part A: Recovery, Utilization and Environmental Effects* 43 (23): 3064–81. <https://doi.org/10.1080/15567036.2020.1833112>.

Sharma, Abhishek, Yashvir Singh, Nishant Kumar Singh, Amneesh Singla, Hwai Chyuan Ong, and Wei Hsin Chen. 2020. “Effective Utilization of Tobacco (*Nicotiana Tabaccum*) for Biodiesel Production and Its Application on Diesel Engine Using Response Surface Methodology Approach.” *Fuel* 273 (August). <https://doi.org/10.1016/j.fuel.2020.117793>.

Sharma, Abhishek, Yashvir Singh, Avdhesh Tyagi, and Nishant Singh. 2020. “Sustainability of the Polanga Biodiesel Blends during the Application to the Diesel Engine Performance and Emission Parameters—Taguchi and RSM Approach.” *Journal of the Brazilian Society of Mechanical Sciences and Engineering* 42 (1). <https://doi.org/10.1007/s40430-019-2102-3>.

Singh, Aparna, Shailendra Sinha, and Akhilesh Kumar Choudhary. 2021. “Optimization of Operating Parameters of Diesel Engine Powered with *Jatropha* Oil Diesel Blend by Employing Response Surface Methodology.” *International Journal of Renewable Energy Research* 11 (2): 504–13. <https://doi.org/10.20508/ijrer.v11i2.11808.g8172>.

Singh, Mandeep, and Sarbjot Singh Sandhu. 2021. “Effect of Boost Pressure on Combustion, Performance and Emission Characteristics of a Multicylinder CRDI Engine Fueled with Argemone Biodiesel/Diesel Blends.” *Fuel* 300 (September): 121001. <https://doi.org/10.1016/j.fuel.2021.121001>.

Sreedhar, C., and B. Durga Prasad. 2015. “Investigating on Use of Different Blends of White

- Grape Seed Biodiesel and Diesel on 4-Stroke Single Cylinder DI Diesel Engine.” *Int. J. Eng. Res. Appl.* 5 (2): 18–23.
- Teoh, Yew Heng, Heoy Geok How, Farooq Sher, Thanh Danh Le, Hwai Chyuan Ong, Huu Tho Nguyen, and Haseeb Yaqoob. 2021. “Optimization of Fuel Injection Parameters of Moringa Oleifera Biodiesel-Diesel Blend for Engine-out-Responses Improvements.” *Symmetry* 13 (6). <https://doi.org/10.3390/sym13060982>.
- USLU, Samet, and Murat Kadir YEŞİLYURT. 2020. “Improving the Running Conditions of Diesel Engine with Grape Seed Oil Additives by Response Surface Design.” *International Journal of Automotive Science And Technology* 4 (3): 185–92. <https://doi.org/10.30939/ijastech..770058>.
- Venkatesan, Hariram, Bose A, and Seralathan Sivamani. 2022. “Evaluating the Predicting Capability of Response Surface Methodology on Biodiesel Production from Grape Seed Bio-Oil.” *Energy Sources, Part A: Recovery, Utilization and Environmental Effects* 44 (1): 2473–88. <https://doi.org/10.1080/15567036.2019.1649759>.
- Arul Peter, A., M. Chandrasekaran, P. Prakash, T. Vinod Kumar, and P. Vivek. 2020. “Experimental Investigation of a Spark Ignition Engine Using Blends of Biogas.” *International Journal of Ambient Energy* 41 (4): 462–65. <https://doi.org/10.1080/01430750.2018.1472656>.
- Prakash, P, and C Dhanasekaran. 2022. “Application of ANN, RSM on Engine Response Prediction Using Lemongrass Biomaterial Blends.” *Materials Today: Proceedings* 69 (xxxx): 684–88. <https://doi.org/10.1016/j.matpr.2022.07.116>.
- Prakash, Paramasivam, and Chinnathambi Dhanasekaran. 2023. “Influencing Parameter Optimisation of CRDI Engine Fuelled with Lemongrass Biodiesel Blends.” *International Journal of Ambient Energy* 44 (1): 719–38. <https://doi.org/10.1080/01430750.2022.2142286>.
- Venkatesan, Hariram, Seralathan Sivamani, Srinivasan Sampath, V. Gopi, and M. Dinesh Kumar. 2017. “A Comprehensive Review on the Effect of Nano Metallic Additives on Fuel Properties, Engine Performance and Emission Characteristics.” *International Journal of Renewable Energy Research* 7 (2): 825–43. <https://doi.org/10.20508/ijrer.v7i2.5678.g7064>.

- A.R.Sivaram , N.Prabhu , P.Ramanathan , R.Rajavel , P.Prakash, Investigation of Pongamia Pinnata with Nano Additives on Performance Characteristics of Diesel Engine, TEST Engineering & Management, ISSN: 0193-4120 Page No. 14332 – 14338, 21 April 2020. <http://www.testmagzine.biz/index.php/testmagzine/article/view/6278>.
- P.Prakash, C.Dhanasekaran, Experimental investigation on Jatropha-methanol blends in direct injection diesel engines, in international journal of vehicle structure & systems, Dec 2019 <http://maftree.org/eja/index.php/ijvss/article/view/1273>
- Abbas, Munawar, and Nargis Khan. 2023. “Numerical Study for Bioconvection in Marangoni Convective Flow of Cross Nanofluid with Convective Boundary Conditions.” *Advances in Mechanical Engineering*. SAGE Publications Inc. <https://doi.org/10.1177/16878132231207625>.
- Abbas, M., Khan, N., Hashmi, M.S. et al. Scrutinization of marangoni convective flow of dusty hybrid nanofluid with gyrotactic microorganisms and thermophoretic particle deposition. *J Therm Anal Calorim* 149, 1443–1463 (2024). <https://doi.org/10.1007/s10973-023-12750-9>
- Afzal, Asif, Roji George Roy, Chacko Preno Koshy, Alex Y, Mohamed Abbas, Erdem Cuce, Abdul Razak RK, Saboor Shaik, and C. Ahamed Saleel. 2023. “Characterization of Biodiesel Based on Plastic Pyrolysis Oil (PPO) and Coconut Oil: Performance and Emission Analysis Using RSM-ANN Approach.” *Sustainable Energy Technologies and Assessments* 56 (December 2022): 103046. <https://doi.org/10.1016/j.seta.2023.103046>.
- Aneeqe, Mohammed, Saad Alshahrani, Mohammed Kareemullah, Asif Afzal, C Ahamed Saleel, Manzoore Elahi M Soudagar, Nazia Hossain, Ram Subbiah, and Mohamed H Ahmed. 2021. “The Combined Effect of Alcohols and Calophyllum Inophyllum Biodiesel Using Response Surface Methodology Optimization.” *Sustainability* 13: 7345. <https://doi.org/https://doi.org/10.3390/su13137345>.
- Arunkumar, Munimathan, Vinayagam Mohanavel, Asif Afzal, Thanikodi Sathish, and Manickam Ravichan-. 2021. “A Study on Performance and Emission Characteristics of Diesel Engine Using Ricinus Communis (Castor Oil) Ethyl Esters.” *Energies* 14: 4320. <https://doi.org/https://doi.org/10.3390/en14144320>.

- Huddar, Vivekanand B, Abdul Razak, Erdem Cuce, Sudarshana Gadwal, Mamdooh Alwetaishi, Asif Afzal, C Ahamed Saleel, and Saboor Shaik. 2022. "Thermal Performance Study of Solar Air Dryers for Cashew Kernel : A Comparative Analysis and Modelling Using Response Surface Methodology (RSM) and Artificial Neural Network (ANN)." *International Journal of Photoenergy* 2022. <https://doi.org/https://doi.org/10.1155/2022/4598921>.
- Khandal, S. V., Abdul Razak, Ibhram Veza, Asif Afzal, Mamdooh Alwetaishi, Saboor Shaik, Ümit Ağbulut, and Ahmad Rashedi. 2022. "Hydrogen and Dual Fuel Mode Performing in Engine with Different Combustion Chamber Shapes: Modelling and Analysis Using RSM-ANN Technique." *International Journal of Hydrogen Energy*, no. xxxx. <https://doi.org/10.1016/j.ijhydene.2022.09.193>.
- Chellakumar, I. J. R. L. J. S., Jida, S. N., Megiso, T. D., Venkatesan, E. P., & Sanipina, A. (2023). Improving output parameters of eco-friendly bio fueled diesel engine by swirling grooves piston design. In *AIP Conference Proceedings. PROCEEDINGS OF INTERNATIONAL CONFERENCE ON INNOVATIONS IN CIVIL ENGINEERING-ICICE 2022*. AIP Publishing. <https://doi.org/10.1063/5.0165295>
- Marisetti, B. R., Dash, S. K., & Janaki, D. V. (2023). Experimental investigation of a diesel engine fuelled by graphene nano particle blended sapota biodiesel. In *IWOSP 2021, INTERNATIONAL WORKSHOP ON STATISTICAL PHYSICS. IWOSP 2021, INTERNATIONAL WORKSHOP ON STATISTICAL PHYSICS*. AIP Publishing. <https://doi.org/10.1063/5.0134418>
- Mahesha, C. R., Rani, G. J., Dattu, V. S. N. C. H., Rao, Y. K. S. S., Madhusudhanan, J., L., N., Sekhar, S. C., & Sathyamurthy, R. (2022). Optimization of transesterification production of biodiesel from *Pithecellobium dulce* seed oil. In *Energy Reports (Vol. 8, pp. 489–497)*. Elsevier BV. <https://doi.org/10.1016/j.egy.2022.10.228>
- Shaarani, S. M., Ramli, A. N. M., Manas, N. H. A., Ahmad, R. A., Fuzi, S. F. Z. M., & Arshad, Z. I. M. (2023). Biofuel scale-up from waste source and strategies for cost optimization. In *Valorization of Wastes for Sustainable Development (pp. 155–180)*. Elsevier. <https://doi.org/10.1016/b978-0-323-95417-4.00007-x>
- Elumalai, R., Sumathy, S., K, R., Akhtar, M. N., P V, E., Khan, S. A., Gupta, M. S., & Asif, M. (2024). Experimental investigation and gray relational optimization of engine parameters to improve the output characteristics of an ammonia biodiesel powered dual fuel combustion

- engine. In *Case Studies in Thermal Engineering* (Vol. 56, p. 104197). Elsevier BV. <https://doi.org/10.1016/j.csite.2024.104197>
- Abbas, M., Khan, N., Hashmi, M. S., & Inc, M. (2023). Aspects of chemical reaction and mixed convection in ternary hybrid nanofluid with Marangoni convection and heat source. In *Modern Physics Letters B* (Vol. 38, Issue 20). World Scientific Pub Co Pte Ltd. <https://doi.org/10.1142/s0217984924501616>
- Abbas, M., Khan, N., Alshomrani, A. S., Hashmi, M. S., & Inc, M. (2023). Performance-based comparison of Xue and Yamada–Ota models of ternary hybrid nanofluid flow over a slendering stretching sheet with activation energy and melting phenomena. In *Case Studies in Thermal Engineering* (Vol. 50, p. 103427). Elsevier BV. <https://doi.org/10.1016/j.csite.2023.103427>
- Abbas, M., Khan, N., Hashmi, M.S. et al. Numerically analysis of Marangoni convective flow of hybrid nanofluid over an infinite disk with thermophoresis particle deposition. *Sci Rep* 13, 5036 (2023). <https://doi.org/10.1038/s41598-023-32011-x>
- Abbas, M., Khan, N., Hashmi, M.S. et al. Numerical analysis of Marangoni convective flow of gyrotactic microorganisms in dusty Jeffrey hybrid nanofluid over a Riga plate with Soret and Dufour effects. *J Therm Anal Calorim* 148, 12609–12627 (2023). <https://doi.org/10.1007/s10973-023-12549-8>
- Abbas, M., Khan, N., Hashmi, M. S., Alotaibi, H., Khan, H. A., Rezapour, S., & Inc, M. (2024). Importance of thermophoretic particles deposition in ternary hybrid nanofluid with local thermal non-equilibrium conditions: Hamilton–Crosser and Yamada–Ota models. In *Case Studies in Thermal Engineering* (Vol. 56, p. 104229). Elsevier BV. <https://doi.org/10.1016/j.csite.2024.104229>

Journal Pre-proof

P.Prakash - Writing- Reviewing and Editing, Elumalai PV - Funding acquisition, Hariharan Chelladurai - Formal analysis, Golden Renjith Nimal Renjith Josephine - Methodology Ramesh Velumayil - Data curation Mohammad Asif & Chan Choon Kit - Supervisor Balambica Venkatesan - Resources Sabarish Rajagopal - Resources Baskar -Visualization Sanjeevi, M. Venkateswar Reddy - Investigation Prabhakar S - Validation

Journal Pre-proof

Declaration of interests

The authors declare that they have no known competing financial interests or personal relationships that could have appeared to influence the work reported in this paper.

The authors declare the following financial interests/personal relationships which may be considered as potential competing interests:

Mohammad Nishat Akhtar reports financial support was provided by Universiti Sains Malaysia. If there are other authors, they declare that they have no known competing financial interests or personal relationships that could have appeared to influence the work reported in this paper.

Journal Pre-proof